

PULL-OUT TEST OF GROUTED ROCK BOLTS AS AFFECTED BY
LOADING RATE AND CURING TIME



A Thesis Submitted in Partial Fulfillment of the Requirements for the
Degree of Master of Engineering in Civil, Transportation
and Geo-Resources Engineering
Suranaree University of Technology
Academic Year 2022

การทดสอบกำลังรับแรงดึงของหมุดยึดหินที่มีผลกระทบจากอัตราการให้แรง
และระยะเวลาบ่ม



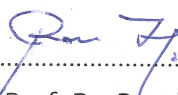
นายปิยวัฒน์ อภิชัยบุคคล

วิทยานิพนธ์นี้เป็นส่วนหนึ่งของการศึกษาตามหลักสูตรปริญญาวิศวกรรมศาสตรมหาบัณฑิต
สาขาวิชาวิศวกรรมโยธา ขนส่ง และทรัพยากรธรณี
มหาวิทยาลัยเทคโนโลยีสุรนารี
ปีการศึกษา 2565

PULL-OUT TEST OF GROUTED ROCK BOLTS AS AFFECTED BY LOADING RATE AND CURING TIME

Suranaree University of Technology has approved this thesis submitted in partial fulfillment of the requirements for a Master's Degree.

Thesis Examining Committee



.....
(Assoc. Prof. Dr. Pornkasem Jongpradist)
Chairperson



.....
(Asst. Prof. Dr. Decho Phueakphum)
Member (Thesis Advisor)



.....
(Asst. Prof. Dr. Prachya Tepnarong)
Member



.....
(Assoc. Prof. Dr. Chatchai Jothityangkoon)
Vice Rector for Academic Affairs and
Quality Assurance



.....
(Assoc. Prof. Dr. Pornsiri Jongkol)
Dean of Institute of Engineering

ปริญญานิพนธ์ อภิชาติบุคคล : การทดสอบกำลังรับแรงดึงของหมุดยึดหินที่มีผลกระทบจากอัตราการให้แรงและระยะเวลาบ่ม (PULL-OUT TEST OF GROUTED ROCK BOLTS AS AFFECTED BY LOADING RATE AND CURING TIME) อาจารย์ที่ปรึกษา : ผู้ช่วยศาสตราจารย์ ดร.เดโช เผือกภูมิ, 68 หน้า.

คำสำคัญ : PULL-OUT TEST/EFFECT OF CURING TIME/LOADING RATE/ROCK BOLT

จุดมุ่งหมายของการศึกษาในครั้งนี้ คือ การประเมินผลกระทบจากอัตราแรงดึงที่มีผลต่อประสิทธิภาพแรงเฉือนของซีเมนต์ที่อุดในหิน ตัวอย่างหินที่นำมาทดสอบแรงดึงในการศึกษาครั้งนี้ถูกเตรียมขึ้นจากหินทรายพระวิหารโดยมีขนาด $110 \times 110 \times 200$ ลูกบาศก์มิลลิเมตร หลุมเจาะขนาดเส้นผ่านศูนย์กลางขนาด 25 มิลลิเมตร สำหรับติดตั้งหมุดยึดขนาดเส้นผ่านศูนย์กลาง 12 มิลลิเมตร ถูกเตรียมที่ตรงกลางตัวอย่างหิน วัสดุในการเกราท์เตรียมจากปูนซีเมนต์ปอร์ตแลนด์เกรดอุตสาหกรรม (ประเภท 1) ผสมกับน้ำและทราย ที่อัตราส่วน น้ำ-ซีเมนต์ เท่ากับ 0.45 และ ซีเมนต์-ทราย เท่ากับ 1:1 หมุดยึดและวัสดุเกราท์จะถูกติดตั้งไว้ในหลุมเกราท์โดยมีระยะการฝังเท่ากับ 100 มิลลิเมตร ทำการบ่มในน้ำเป็นเวลา 7, 14, 21, และ 28 วัน ก่อนนำไปทำการทดสอบ เครื่องมือการทดสอบกำลังรับแรงดึงถูกสวมเข้ากับหมุดยึดและถูกประยุกต์ใช้ในการดึงด้วยอัตราแรงดึงที่แตกต่างกัน ตั้งแต่ 0.0001, 0.001, 0.01 ถึง 0.1 มิลลิเมตร/วินาที สำหรับค่ากำลังอัดในแนวแกนเดียวของวัสดุเกราท์จะถูกทดสอบที่แต่ละช่วงระยะเวลาการบ่ม ผลการทดสอบระบุว่า กำลังรับแรงดึงมีค่าสูงขึ้นตามระยะเวลาการบ่มที่นานขึ้น โดยอัตราการให้แรงที่เร็วขึ้นจะให้ค่าแรงดึงมีค่าสูงกว่าในอัตราการให้แรงที่ช้า ในขณะที่ระยะเวลาเคลื่อนตัวในอัตราการให้แรงที่ช้าจะให้ระยะที่มากกว่าอัตราการให้แรงที่เร็วกว่า โดยการวิบัติได้แบ่งเป็นสองรูปแบบ ได้แก่ โชนหมุดยึดหิน-วัสดุเกราท์ และโชนวัสดุเกราท์-หิน กำลังรับแรงกดในแนวแกนเดียวของซีเมนต์เกราท์มีค่าเพิ่มขึ้นถึง 80% ในช่วงระหว่างสัปดาห์แรก สูตรความสัมพันธ์ทางคณิตศาสตร์ระหว่างค่ากำลังรับแรงดึงสูงสุดกับระยะเวลาการบ่มถูกคิดขึ้นเพื่อใช้ในการทำนายประสิทธิภาพแรงเฉือนของซีเมนต์ที่อุดภายในหิน

สาขาวิชา เทคโนโลยีธรณี
ปีการศึกษา 2565

ลายมือชื่อนักศึกษา Pim
ลายมือชื่ออาจารย์ที่ปรึกษา Dr. Phuatphum

PIYAWAT APICHAIBUKKHON : PULL-OUT TEST OF GROUTED ROCK BOLTS AS AFFECTED BY LOADING RATE AND CURING TIME. THESIS ADVISOR : ASST. PROF. DECHO PHUEAKPHUM, Ph.D., P.E. 68 PP.

Keyword : PULL-OUT TEST/EFFECT OF CURING TIME/LOADING RATE/ROCK BOLT

The aim of this study is to assess the effect of pull-out rate on the shear resistance of cement plug in rocks. The rock specimens for pull-out testing in this study are prepared from Phra Wihan sandstone to have nominal dimensions of 110×110×200 mm³. A 25-mm diameter of pre-drilling hole along the centerline of rock specimens are prepared for installing a 12-mm diameter rebar bolt. The grouting material is prepared from commercial grade Portland cement mixed (Type 1) with water-cement and sand-cement ratio of 1:0.45 and 1:1. The rebar bolt and grouting material are installed in the grouting hole with an embedment length of 100 mm then left to cure for 7, 14, 21, and 28 days in water before testing. The rock bolt pull-out test apparatus is equipped with a rebar bolt to apply different pull-out rates from 0.0001 0.001 0.01 to 0.1 mm/sec. Uniaxial compressive strengths of grouting materials are examined for each curing period. Test results indicate that pull-out strength is higher with longer curing time. The high pull-out rate leads to higher pull-out strength than the low rate while displacement at low rate is more than a high rate. The failure patterns can be divided into two groups: rock bolt-grout zone and grout-rock zone. Uniaxial compressive strength of grout rapidly increases to 80% during first week. Mathematical relation between the maximum pull-out strength and curing time is formulated to predict shear resistance of cement plug in rocks.

School of Geotechnology
Academic Year 2022

Student's Signature *ปิยวัฒน์*
Advisor's Signature *D. Phueakphum*

ACKNOWLEDGEMENTS

I am very grateful for the support of the scholarship and this research from Suranaree University of Technology (SUT) and the faculty who have given me the opportunity and scholarship.

I would like to express my deepest gratitude to Assistant Professor Dr. Decho Phueakphum for the advice, investigation, and correction. I am proud and truly appreciate those things. I would like to thank Assoc. Prof. Dr. Pornkasem Jongpradist and Asst. Prof. Dr. Prachya Tepnarong for their thesis committees for providing honest criticism and guidance on my research. Special thanks to the Geomechanics Research Unit (GMR), especially Prof. Dr. Kittitep Fuenkajorn and Dr. Thanittha Thongrapha, who helped with equipment and tools in conducting the research as well as providing suggestions and various concepts, including friends, brothers, and sisters in the department or the persons who assisted and the research laboratory (F4) in this study.

Finally, I would like to thank my affectionate parents for giving me a good treat and promoting education very well all along, and always encouraging me until I graduated.

Piyawat Apichaibukkhon

มหาวิทยาลัยเทคโนโลยีสุรนารี

TABLE OF CONTENTS

	Page
ABSTRACT (THAI).....	I
ABSTRACT (ENGLISH).....	II
ACKNOWLEDGEMENTS.....	III
TABLE OF CONTENTS.....	IV
LIST OF TABLES.....	VI
LIST OF FIGURES.....	VII
SYMBOLS AND ABBREVIATIONS.....	X
CHAPTER	
1. INTRODUCTION.....	1
1.1 Background and rationale.....	1
1.2 Research objectives.....	2
1.3 Research methodology.....	2
1.3.1 Literature review.....	3
1.3.2 Sample collection and preparation.....	3
1.3.3 Laboratory test	3
1.3.4 Analysis and comparisons.....	4
1.3.5 Discussion and conclusion.....	4
1.3.6 Thesis writing.....	4
1.4 Scope and limitations.....	4
1.5 Thesis contents.....	4
2. LITERATURE REVIEW.....	6
2.1 Introduction.....	6
2.2 Failure mechanism of grouted bolt.....	6
2.3 Failure modes of two phase material system.....	7
2.4 Effect of reinforcing on pull-out test.....	8
2.5 Factor effect on performance of rock bolt.....	10
2.5.1 Composition.....	10
2.5.2 Curing time.....	11
2.5.3 Stress field condition.....	12

TABLE OF CONTENTS (Continued)

	Page
2.5.4 Rock properties.....	13
2.5.5 Drill hole characteristics.....	14
2.5.6 Size effect.....	15
2.5.7 Bolt properties.....	16
2.5.8 Grout properties.....	16
2.5.9 Loading rate.....	19
2.6 Energy absorption.....	21
3. SAMPLE PREPARATION.....	25
3.1 Introduction.....	25
3.2 Natural sand.....	25
3.3 Portland cement.....	26
3.4 Sandstone sample and rock bolt.....	29
4. LABORATORY TESTING.....	32
4.1 Introduction.....	32
4.2 Uniaxial compression test.....	32
4.3 Pull-out test.....	37
5. DERIVATION OF EMPIRICAL EQUATIONS.....	46
5.1 Introduction.....	46
5.2 Pull-out load as a function of curing time.....	46
5.3 Displacement as a function of curing time.....	47
6. DISACUSSIONS, CONCLUSION, AND RECOMMENDATIONS FOR FUTURE STUDIES.....	49
6.1 Discussions.....	49
6.2 Conclusions.....	51
6.3 Recommendations for the future studies.....	52
REFERENCES.....	53
APPENDIX A LIST OF PUBLICATIONS.....	59
BIOGRAPHY.....	68

LIST OF TABLES

Table	Page
2.1 The influence of the water to cement ratio on the bolt bond strength (Kilic et al, 2002)	17
3.1 List of specimen number, length, diameter, weight, ratio of length/diameter and density.....	28
3.2 List of number specimen, grout type, diameter bolt, diameter hole, embedment length, and ratio of embedment length/diameter.....	31
4.1 Uniaxial compressive strength (σ_c), elastic modulus, and Poisson ratio of cement grouting in the curing time function.....	34
4.2 Tests results under different loading rates with pull-load and maximum displacement as a function of curing time.....	40
4.3 Failure modes observed for the post-test specimens.....	45

LIST OF FIGURES

Figure		Page
1.1	Research Methodology.....	2
2.1	Rock bolt installed in rock joint (Minova, 2006)	8
2.2	Composite support reaction lines. (a) Case 1: different support elements installed at the same time after tunnel excavation. (b) Case 2: different support element installed at different times after tunnel excavation (Kim et al, 2019)	11
2.3	The effect of the grout's setting time on pull-out strength of rock bolt in (a) moderate rock and (b) weathered rock (Kim et al, 2019)	12
2.4	Effect of confining pressure on borehole surrounding rock mass during pull-out test: (a) low confining stress ($\sigma_2 = \sigma_3$), (b) high confining stress ($\sigma_2 = \sigma_3$), and (c) confining stress ($\sigma_2 \neq \sigma_3$) (Kim et al, 2019)	13
2.5	The optimal range between hole diameter and rock bolt diameter (Ghazvinian and Rashidi, 2010)	15
2.6	The relationship between grout of shear strength, uniaxial compressive strength, and bond strength (Kilic et al, 2002)	18
2.7	Bearing capacity in the ground reaction curve (Hao et al, 2020)	22
2.8	Deformation curve of moving and energy daily absorption in the roadway by measuring micro seismic wave (Dai et al, 2018)	23
2.9	Sample of Paddle – anchor during testing until after testing (Li, 2010).....	24
3.1	Sieve size number 20 and 40 sorted natural sand.....	26
3.2	Portland Cement Type 1 is used in this study.....	27
3.3	Mixer, Kitchenaid Professional 600 6QT 575 watts stand mixer,	

LIST OF FIGURES (Continued)

Figure	Page
with maximum capacity of 5,000 cc and 6 speed control.....	27
3.4 Casing grout specimen in PVC tube for compression test.....	27
3.5 Sandstone specimen with dimension 110x110x200 mm ³ by saw cut surface and drilled with 25 mm diameter hole.....	30
3.6 Deformed bar with 12 mm diameter for pull-out test.....	30
3.7 Heater bypass cap for plugging grouting material.....	30
4.1 Some grouting specimens with ratio of L/D = 2.0 prepared for uniaxial compression test.....	33
4.2 Test arrangement and apparatus for the uniaxial compressive strength test on the cylindrical shape cement-grout specimen.....	33
4.3 Uniaxial compressive strengths as a function of curing times.....	35
4.4 Poisson's ratio as a function of curing times.....	35
4.5 Elastic modulus as a function of curing times.....	36
4.6 Some post-test specimens were obtained from the uniaxial compression test on the cement-grout sample when cured for 3, 7, 14, 21, and 28 days.....	36
4.7 Sample preparation for pull-out test.....	37
4.8 Pull-out test apparatus and test set up for pull-out test.....	38
4.9 Load-displacement curve obtained for 7, 14, 21, and 28 days of curing samples under various loading rates. The cross symbols represent the ultimate pull-out load for such loading rate.....	39
4.10 Peak load of pull-out test as a curing times function.....	41
4.11 Displacement of pull-out test as a curing times function.....	41

LIST OF FIGURES (Continued)

Figure	Page
4.12 Post-test specimens obtained for the 7 days of curing samples under various loading rates.....	42
4.13 Post-test specimens obtained for the 14 days of curing samples under various loading rates.....	42
4.14 Post-test specimens obtained for the 21 days of curing samples under various loading rates.....	43
4.15 Post-test specimens obtained for the 28 days of curing samples under various loading rates.....	43
4.16 Classification of failure modes that can occur during the pull-out test.....	44
5.1 Comparison peak load between pull-out test and empirical equation as a curing time function.....	47
5.2 Comparison displacement between pull-out test and empirical equation as a curing time function.....	48

SYMBOLS AND ABBREVIATIONS

ν	=	Poisson' ratio
\dot{d}_s	=	Loading rate
a	=	Empirical parameters
A_b	=	Cross-sectional area of bolt
b	=	Empirical parameters
c	=	Empirical parameters
C:S	=	Cement to sand ratio
D	=	Pull-out displacement
d_b	=	Bolt diameter
D_{Bolt}	=	Diameter of bolt
D_{Hole}	=	Diameter of grouting hole
E	=	Elastic modulus
e	=	Empirical parameters
K_i	=	Reinforcement stiffness
K_{total}	=	Total stiffness
L/D	=	Length to diameter ratio
l_b	=	Bolt length
P	=	Maximum or Ultimate pull-out load
P_b	=	Maximum pull-out load of the bolt
P_{max}	=	Maximum compressive load
s/c	=	Sand to cement ratio
t	=	Curing time

SYMBOLS AND ABBREVIATIONS (Continued)

UCS_g	=	Uniaxial compressive strength of grout material
w/c	=	Water to cement ratio
$W:C$	=	Water to cement ratio
α	=	Empirical constants
γ	=	Empirical constants
δ	=	Empirical constants
ε	=	Empirical constants
ζ	=	Empirical constants
θ	=	Empirical constants
κ	=	Empirical constants
λ	=	Empirical constants
π	=	Pi
ρ	=	Density
σ_2	=	Uniaxial compressive strength
τ_b	=	Bolt bond strength
τ_g	=	Shear strength of grout material
$^{\circ}C$	=	Degree Celsius

CHAPTER 1

INTRODUCTION

1.1 Background and rationale

There are many types of support in rock mass. One of the support systems is rock bolt support. It has been used in civil and mining projects that involve surface and underground excavations in rock masses, such as tunnels, rock slopes, and foundations. They are widely used to improve stability and maintain the load-bearing capacity of rock near the excavation boundaries. There are many potential factors affecting the durability and the performance of rock bolts, including rock mass characteristics (strength and creep behavior of rock), bolt parameters (bolt type, tensile strength, elongation, corrosion, bolt length, and diameter), grout material (grout types, mixture, and water-to-cement ratio), and anchorage system (embedment length, hole diameter to bolt diameter ratio, number of bolts, bolt spacing and orientation of rock bolt (Frenelus et al., 2022). In dam construction, the water which water weight is modified according to the temperature and hydropower lead to action force subjected to the internal and external hydrostatic load. The pressure will start coming influence when the dam surface has occurred the initial crack. The compression load and shear stress act with zero stress and maximum stress on the toe of dam, respectively. The changing of water level in the headwater leads to stress conversion and occurring failure (tip crack and uplift failure) where occur area of the dam, foundation, and plane's contact with the foundation (Federal Energy Regulatory Commission, 2002). Likewise, wind velocity affects the wind turbine. The aerodynamic load executes on the structure to the tower bottom with increased stress as the wind rate increases (Wang et al., 2013). Many researchers have carried out laboratory tests, field tests, analytical methods, and numerical analysis for a better understanding of rock bolt performance (Ghazvinian and Rashidi, 2010; Li et al., 2016; Chen, 2014; Hyett et al., 1992; Chen and Li, 2015; Yang, 2022; Zhang et al., 2020; Høien et al., 2021; Li et al., 2017). Even though several factors have been tested, the performance of cement plugs in rocks as affected by the pull-out rate and curing time has been rare and used to prevent hazardous conditions such as the collapse of buildings, tower overturning, or high structures related to tension foundations.

1.2 Research objectives

The objectives of this study are to assess the effect of pull-out rate of shearing resistance of cement plug in rocks. The pullout test is performed on Phra Wihan sandstone specimens. Different loading rates are used to pull-out the steel bar from a test hole. A mathematical relation between the maximum pull-out strength and displacement will be formulated to predict the shear performance of cement plug in rocks as function of curing time and loading rate. The findings will improve understanding of the shearing resistance of cement plug in rocks under different pull-out rates and curing time for rock support.

1.3 Research methodology

The research methodology shown in Figure 1.1 comprises 6 steps; including literature review, samples collection and preparation, Laboratory test, result analysis and comparison, discussions and conclusions, and thesis writing.

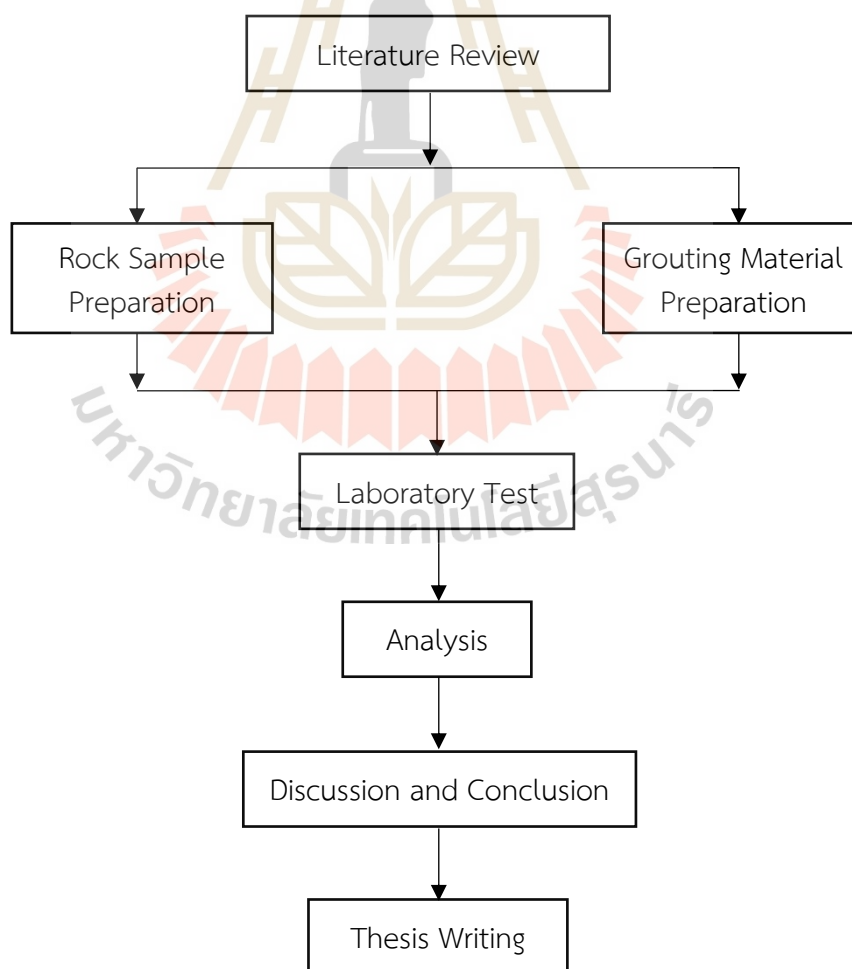


Figure 1.1 Research Methodology

1.3.1 Literature review

Literature review is carried out to study researches about the standard testing procedure of pull-out test, pull-out test on grouted rock bolts in laboratory, the influencing parameters on shear resistant of grouted rock bolt and the relevant theory of pull-out test. The sources of information are from text books, journals, technical reports and conference papers. A summary of the literature review is given in the thesis.

1.3.2 Sample collection and preparation

The rock specimen use here is prepared from Phra Wihan sandstone to has nominal dimensions of $110 \times 110 \times 200 \text{ mm}^3$ in the laboratory at the Suranaree University of Technology, Nakhon Ratchasima province. A 25 mm diameter of predrilling hole along the centerline of rock specimens will be prepared for installing a 12 mm diameter rebar bolt. The uniaxial compressive strength of the grouted material is determined by testing cylinder specimens that diameter and length were $54 \times 108 \text{ mm}$ in size ($L/D = 2.0$) for each curing time period of 3, 7, 14, 21, and 28 days. Grouting material is cement grout. The cement grout is prepared from the commercial grade Portland cement (Type 1) mixed with water-cement and sand-cement ratio of 0.45:1 and 1:1. The rebar bolt and grouting material are installing in the grouting hole with an embedment length of 100 mm then left to cure for 7, 14, 21, and 28 days by submerging in water before testing.

1.3.3 Laboratory test

The rock bolt pullout test apparatus is used to equip with the rebar bolt and apply the different four pullout rates from 0.0001, 0.001, 0.01 to 0.1 mm/s in accordance with the ASTM standard D4435-13 and suggestion method from ISRM suggested methods for rock bolt testing. The slowest speed gives appropriate time for testing. All testing is made under a dry condition. The rock bolt pullout test apparatus comprises a central hole jack, hand pump with load gauge, directional control valve, flexible pipes and truss high tensile test rod with coupling. In general, the pullout force is indicated on load gauge; however, a load cell can be used for the measuring of pull-out load. An arrangement is provided for fixing the dial gauge for estimating displacement against the load. The axial displacement and pull-out load will be recorded during testing until failure occur.

1.3.4 Analysis and comparisons

The mathematical relation between the maximum pull-out levels and pullout rates under function of curing times is formulated to predict the shear performance of fully grouted rock bolt. The research findings is published in conference paper or journal.

1.3.5 Discussion and conclusion

The reliability and suitability of discussion will be identified and used to performance evaluation. The thesis includes research activities, methods, and results. The research or findings is published in the conference proceedings or journals.

1.3.6 Thesis writing

All research activities, methods, and results are documented and complied in the thesis. This research is an application to design pull-out of cement plug which bearing capacity strength parameter of pull-out test.

1.4 Scope and limitations

The scope and limitations of the research include as follows.

- 1) The nominal dimensions of tested specimens are $110 \times 110 \times 200 \text{ mm}^3$.
- 2) The pullout test procedure follows the ASTM D4435-13e1 standard practice and suggestion method from ISRM.
- 3) The cement grout is prepared from the commercial grade Portland cement (Type 1) mixed with water-cement and sand-cement ratio of 0.45:1 and 1:1.
- 4) The sample is tested performed in 5 and 4 periods of uniaxial compression and pull-out test.
- 5) The uniaxial compression is tested under constant rate (1 MPa/s) by following ASTM 7012-14.
- 6) The pulling rates applied from ISRM suggested method for rock bolt testing are varied from 0.0001, 0.001, 0.01 and 0.1 mm/s.
- 7) All testing is made under dry condition.
- 8) The research findings are published in conference paper or journal.

1.5 Thesis contents

Chapter I describes the background and rationale, the objectives, the methodology and scope and limitations of the research. Chapter II summarizes results

of the literature review. Chapter III describes the sample preparation. Chapter IV and V describes the laboratory testing and derivation of empirical equations. Chapter VI discusses and concludes the research results and provides recommendations for future research studies.



CHAPTER 2

LITERATURE REVIEW

2.1 Introduction

This chapter compiles the results of a literature review carried out to understand and develop the failure mechanism and failure mode of grouted bolts, the effect of reinforcing on pull-out tests, and factors affecting the performance of rock bolts following the standard for pull-out tests.

2.2 Failure mechanism of grouted bolt

The excavated tunnel shows some effects on the stability of the surrounding area. Loading those transfers from the reinforcement system and mechanical action which can be explained for the understanding of support system behavior. According to the classification of Stille et al. (1989), the main concept comes from elastic-plastic grouted bolts. Basic mechanisms can be categorized into three elements namely: 1) Rock movement and load transfer from an unstable zone rock to the reinforcing element. Load transfer occur in weak rock to the bolt, 2) Load transfer from unstable region to a stable region. In this case is not equipped bolt head to transfer load from weak rock into direct grouting material, and 3) Transfer of the reinforcing element load to the stable rock mass. This is the normal pulling by wearing nut and end plate for increasing performance of bolt in elastic phase and considering to grouting material. In the fully grouted bolt, load transfer gives a major shear surface from rock to bolt and bolt to rock via grouting material. Shear resistance is the actual bonding between the roughness of the hole and the profile of the bolt surface.

Feng et al. (2017) investigate the distribution of load on steel tubes with passed differential segments of the same total length (30 cm). The segments (5, 7, 9, 10, and 15 cm) are processed and attached by cement grout ($w/c = 0.25$), there is a compressive strength of 30 MPa within one day and 70 MPa within 28 days. The result shows load transfer from the bolt-clamp end to the tube-clamp end, which evidence is shown trace on material grout with the three conditions (decoupling stage, plastic stage, and elastic stage). The failure is separated into 3 types; bolt fracture always occurs when the last segment has a long length (15 cm) due to its ability to resist axial load from the tube-clamp. The bolt has become a first weight barrier that has position failure starting at 10 cm of total length segment by the combination of short segments

(5 + 5 cm, S1-2), whereas the last segment has not enough length (< 15 cm), and the decoupling failure occurs at the tube end. The received peak load and displacement in this failure will be a lower value than the bolt failure, but it has 3-4 oscillations of load before the load drops at the zero point. For clamp detachment is found this case where each segment has length equally. By spreading the load through the bolt rod to part of the weak section, the spiral of the bolt clam is damaged by print scratch and a certain lower load than both bolt failure and decoupling failure.

2.3 Failure modes of two phase material system

By pull-out testing two phases are defined, which comprise a rebar and concrete column (note: there is no grout material) for this study. The bonding forces of rebar distribute through the center core to the rebar surface and pass surrounding media or concrete with radial force. Lutz (1970) divides the component of bonding force that is passed onto rebar into three parts; 1) Chemical adhesion, which is the main bond strength in two types of material attraction between intermolecular on the surface of rebar and grouted cement. However, it has little effect. 2) Friction will occur after slip, during which the forming of cement and rebar is very close. 3) Mechanic interaction, that rib, thread, or interlocking on the rebar surface helps to brace grouting material or considering the roughness of the rebar. The rebar can slip in two ways; 1) Characteristic wedging action that means the concrete is split together by ribs of rebar following slipping of rebar. 2) Lodge (compacted powder) of concrete where it is stuck in the rib spacing by crushing the rib. In addition, even when slip and separation occur, additional external cracks on the surface concrete led to internal cracks that become transverse cracks, and concrete crack rendering has a chance to split. Thus, large axial displacements cannot occur without transverse and longitudinal cracking in the surrounding concrete. Lutz (1970) also outlines the breaking of a concrete beam into small columns as primary cracking, which is the major failure mode, and transverse cracks with dense minor radial cracks from bond slips.

The initial objective of the bolt reinforcement is to reduce displacement of the existing fractures by applying confining stress to the fracture surfaces. In some cases, rock bolts can reduce some residual phases within the moving strata. Rock bolts installed across the bedded, jointed, or fractured strata are capable of resisting axial and shear deformation (Figure 2.1). The fully grouted bolt function can be classified into three parts: tensile load which affects the axial resistance; shear load, which occurs on the shear plane across the bolt; and the combination of both loads. So, failure occurs following the above description of bolt function, which means the failure occurs

for tensile load: Steel failure of the fastener, concrete cone failure, and Pull-out failure of the fastener, and for shear loads: steel failure and concrete crushing with an unbending bolt and the last one is failure of both loads.

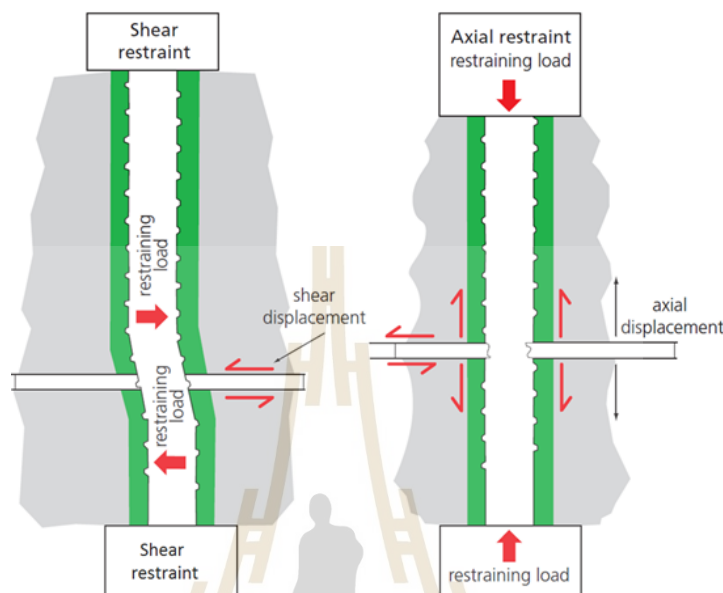


Figure 2.1 Rock bolt installed in rock joint (Minova, 2006).

2.4 Effect of reinforcing on pull-out test

In the study of Thenevin et al. (2017), pull-out test of three rock bolts, including HA25, FRP and SSB rock bolts, are studied. All rock bolts are grouted in sandstone specimens with cementation and resin. The outer surface is installed by a biaxial cell for controlling condition tests under constant radial stiffness (CRS) and constant radial pressure (CRP), but in this study, CRP values of confining have low differential pressure on the curve, therefore CRS grains receive more attention. Load-displacement of HA25, FRP rock bolt occurs in four stages. At the initial stage, interface adhesion, mechanical interlock, and friction encourage the bolt-grout bond. The curve indicates a quasi-linearity. At the secondary stage, the interface develops joints and subsequent curve drops. The load increases until it reaches its maximum value at the third stage. At the fourth stage, residual load on the curve is slowly failing down of HA25 better than FRP because of a higher indentation angle, which causes load-displacement to remain in the residual phase. In the meantime, SSB rock bolts show two peaks response, with the failure in the initial phase being on the bolt-grout interface. Suddenly load drops and a secondary peak is shown by gripping itself against with a smooth surface. For SSB, the residual phase has steady values until the end. Embedment length and confining pressure have been influenced by axial load and displacement when length

and confining pressure have been increased. These include increasing maximum load and bond strength with a smoother curve of FRP than HA25. The maximum load capacity on pull-outs increases with different anchor lengths (Benmokrane et al., 1995) On the other hand, residual load and axial stiffness (load range 40 to 80 kN) are characterized by being non-curved.

Laldji and Young (1988) investigate ground anchorages with different embedment lengths for development. The seven-wire strand is produced in three forms, each of which has the influence in pulling by Stocker and Sozen (1969). The results indicate the increase of the embedment while the tensile force increased, but the displacement of the tensile force level offs have been steady at 0.3 mm slip. The bond stress of a normal strand decreases with increasing embedment. Indented strand has the highest bond stress, more than normal, and dyform strand between free force and 15 N/mm² lateral compression. Although dyform strand has the lowest values but it has the most incremental bond stress for low confining. The tensile force/slip compact (Dyform) strand and normal strand have similar curves in the peak phase and residual phase. For an indented strand to be different in part, residual load increases equal to or greater than peak force. The values of bond stress averaged over all the levels of lateral compression from 0 N/mm³ to 15 N/mm³ are in the following proportions: 1 (normal): 0.9 (Dyform): 1.20.1 (indented). The influence of stress can change bolt performance (MacSporran, 1994).

In the study of Qasem et al. (2020), two types of reinforcing are explored for determining efficient capacity by pull-out test. Carbon fiber resin-forced polymer (CFRP) and steel rebar have been comprised in concrete blocks that can be studied for the behavior of ultra-high-performance-concrete by Yoo and Banthia (2015). The diameters of CFRP and steel rebar are 12 and 16 mm, respectively, for diameter increasing examination. The results show that the bond stress of CFRP is lower than that of steel rebar in the same diameter, with 34.7% and 48.5% on 12 mm and 16 mm diameters, respectively. The personality curve of CFRP and steel rebar is similar in both diameters, but at 12 mm in diameter of CFRP loads have rapid drops until zero in residual stress, rendering end-slip low displacement. Expansion of CFRP diameter which increases bond stress from 1.98 to 2.97 MPa or 44% increasing while steel rebar has been valued from 2.8 MPa to 4.7 MPa, led to an increase of 67% in maximum bond shear stress. With respect to general characteristics, the characteristic of CFRP is no indentation for mechanical support, bearing of stress focuses on friction resistance, unlike steel rebar, where interlocking increases performance of strength and residual

stress, but there are several mechanical parameters and physical advantages for fiber-rebar (Prokeš et al., 2020; Alaoud et al., 2021; Mousavi and Shafei, 2019).

2.5 Factor effect on performance of rock bolt

Empirical classification systems are based on average values from many field tests and conditions. Kim et al. (2019) explore fully grouted-bolt patterns in excavation for tunnel-support. Testing is used in situ to gather rock-mass rating (RMR) systems, rock-quality index (Q) systems, and rock-mass index (RMI) for differential environmental processes. There are several factors that influence the selection of length and diameter bolts, such as tunnel span, rock-mass quality, ground-quality, tunnel size, and block size.

2.5.1 Composition

The compounding of support systems (shotcrete, steel reinforcement, etc.) in grouted rock bolts leads to stiffnesses that combine in the elastic field. The total stiffness can be a sum of each single stiffness, as shown in the equation below:

$$k_{\text{total}} = \sum_i k_i \quad (2.1)$$

where K_{total} = total stiffness of the composite system, and K_i = individual support or reinforcement stiffness. Installation of support at different times affects individual distances from the excavation face, as shown in Figure 2.2. Finally, the combination of every support that varied many processes set up gives the maximum load to close up on the final setting time. The purpose of composite support is to support stability, save cost and adapt the system to environmental conditions.

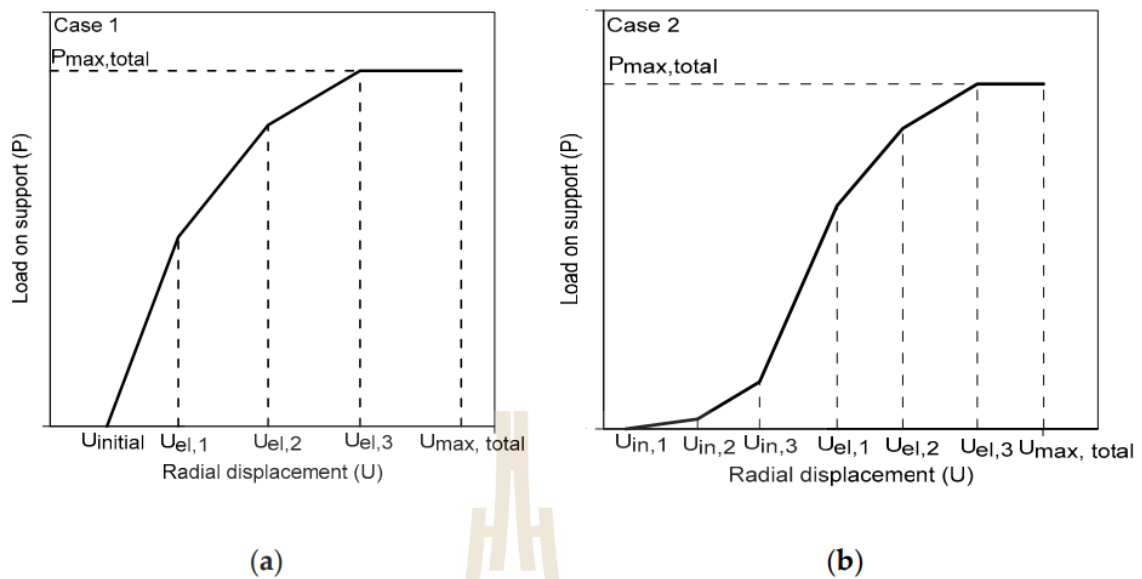


Figure 2.2 Composite support reaction lines (a) Case 1: different support elements installed at the same time after tunnel excavation (b) Case 2: different support elements installed at different times after tunnel excavation (Kim et al., 2019)

2.5.2 Curing time

Fully grouted bolts are based on load transfer type: continuously and mechanically coupled (CMC). There are two groups, although with respect to this experimental study regards on rock bolts are widely consumed in tunneling work and cable bolts are always used in mining operations. Moderate and weather rock are used for 18 pull-out tests for two rock classes under three curing times (12, 24, and 36 hours). The load capacity of both the moderate and weather rocks has increased. In moderate rock, the curing time does not show a significant curve even though the capacity load of each period is greater than that of another type of rock mass, which also affects the gradient in load-displacement curves in weather rock. The inflection points of weather rock have displacement close together with values of 57, 103, and 137 kN for 12, 24, and 36 hours of curing, as shown in Figure 2.3.

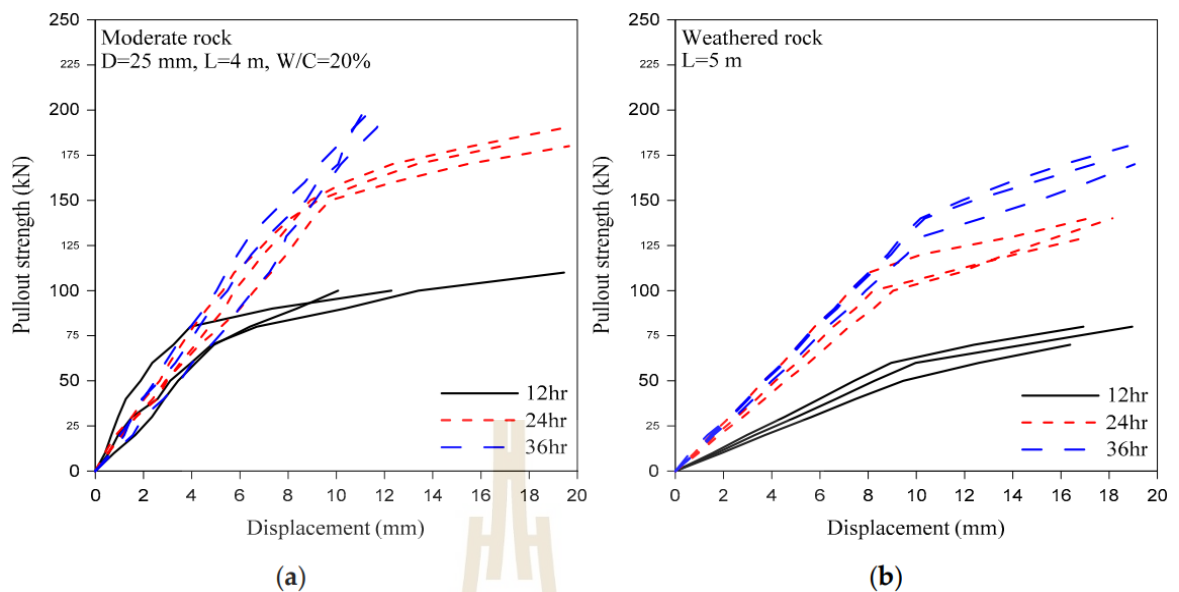


Figure 2.3 The effect of the grout's setting time on pull-out strength of rock bolt in (a) moderate rock and (b) weathered rock (Kim et al, 2019).

Elkhadiri et al. (2009) inspect porosity in the two types of Spanish cement (CEM I 42.5R and CEM II/A-V 42.5) that were cured at a temperature of 4 to 85°C for 2, 7, 15, and 28 days. Both types of cement have the highest compressive strength at a temperature of 85°C with 2 days cured time and decrease with a long-cured time (28 days) because overheating accelerated the reaction to fast ending. Although in the first 7 days, the cements of both types have the highest compressive strength at 40°C, there was a slight decrease after 7 days and remained stable until 28 days, while the temperature of 4°C and 22°C have values increased from 2 to 28 days. The percent of porosity in a few cured times decreases when temperature increases, while a longer cured time reduces similarly porosity except at 85°C. At 40°C give the percent less than other temperatures in minimum and maximum cured time. The X-ray diffraction (XRD) shows the compounding product of hydration (anhydrous phase, hydrate phase, and calcite) below a temperature of 85°C. All products are set molecules and evacuated water/air pores via capillary water described as three main types of water content by Rübner et al. (2010).

2.5.3 Stress field condition

Disturbing stress in depth is an influential factor to exhibit in the role. The Q-system always used in the rock-bolt design. Decreasing confining stress, which is upright along the axial bolt, leads to unstable splitting of the grout and radial fracturing better than in high stress. However, stress in the environment is not

hydrostatic. The minor and major principal stress values have individual crack propagation around the bore hole during the pull-out test, as shown in Figure 2.4. The evolution of the radial fracture streak is broken by parallel major confining pressure in the case of non-hydrostatic pressure.

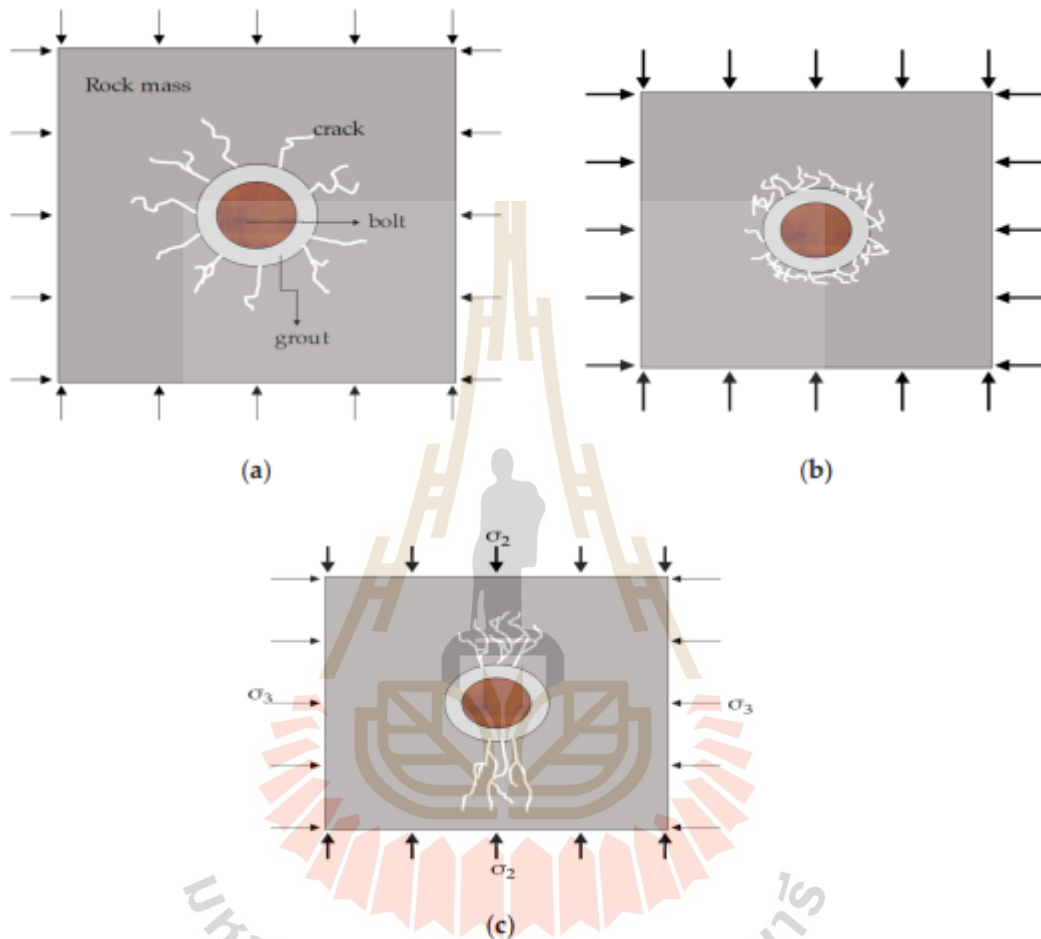


Figure 2.4 Effect of confining pressure on borehole surrounding rock mass during pull-out test: (a) low confining stress ($\sigma_2 = \sigma_3$), (b) high confining stress ($\sigma_2 = \sigma_3$), and (c) confining stress ($\sigma_2 \neq \sigma_3$) (Kim et al, 2019).

2.5.4 Rock properties

The strength of rock mass is one of rock-mass conditions for more or less setup support. Load transfer is a factor passing the rock-mas quality by anchorage performance as inflated steel-tube rock bolts are continuously frictionally coupled (CFC) systems, expansion shell bolts are discretely mechanically or frictionally coupled (DMFC) category, and in this part use CMC systems. Rock mass rating (RMR) is guideline for rock-mass quality; moderate rock; soft rock; and weather rock. The relationship of pull-out strength and the pull-out displacement in

moderate rock are 159.3 kN and 6.29 mm that remain in the range of 14 empirical approach. Soft and weather are 148.8 kN for 8.42 mm and 127.6 kN for 8.545 mm that is low strength than the empirical approach. One thing that is cogitated with compactness in the rock, therefor density is recommended within a parameter in the empirical equation.

Zhai et al. (2016) study varying conditions and variant diameters of the test sample (weak and strong test samples) grouted with two bolt types (MW9 nutcage and Superstrand plain cable bolt). The result shows that the MW9 cable bolt has a higher peak load in the smallest and biggest diameters of the sample (150 and 500 mm) than the Superstrand cable bolt, although the strong test sample has a peak load of about 50 kN higher than the weak test sample. The peak loads in both types of bolts are invariable since they were tested with diameters of 200 and 300 mm in Superstrand and MW9 cable bolts.

Che et al. (2020) establish a bonded-particle contact model (BPM) for pull-out tests by DEM investigation. Simulation of DEM is performed for the multi-layer under compaction method (MUCM) and macroscopic mechanical parameters from several experiments. The sample widths ranged from 40 mm to 400 mm, and the sample heights ranged from 120 mm to 400 mm. The results show the influence of sample width on mechanical properties is substantially greater than that of sample height. Bond breakage occurs for various sample widths, in cases of small sample widths, there is a fracture of grout near the load end, followed by rock near the top of the sample. In large sample width cases, failure occurs along the bolt-grout near the grout-rock interface. The force chain indicates the concentration of two compression forces in the form of an inverted cone at the top with a large width, which means concentrating tension at the bottom. Bond breakage and chain force for various sample heights are important under the same pull-out displacement.

2.5.5 Drill hole characteristics

Normally, a suitable hole is always a cylinder shape to carry out along the bolt length. Ghazvinian and Rashidi (2010) explore the effect of hole diameter on rock bolt diameter. The different bolt diameters (25, 28, and 32 mm) provide different hole diameters (32, 40, 50, 63, and 90 mm). The results indicate that the level of maximum load is between 32 mm and 48 mm diameter holes in a 25 mm diameter rock bolt. In 28 mm and 32 mm diameter rock bolts, there is a range between 47 mm and 55 mm and 54 mm and 62 mm diameter holes, if the diameter

holes have more than this range, the maximum load will decrease by about 5% to 10%, so the hole diameter should be 1.7 to 1.9 times the rock bolt diameter. The optimal range shows two linear equations, as shown in Figure 2.5. Failure of increasing hole diameter occurs on the bolt surface and cement grout, while less hole diameter occurs on the rock surface and cement grout surrounding the hole. Because of the area between the hole and grouting, there is more contact to attach the surface.

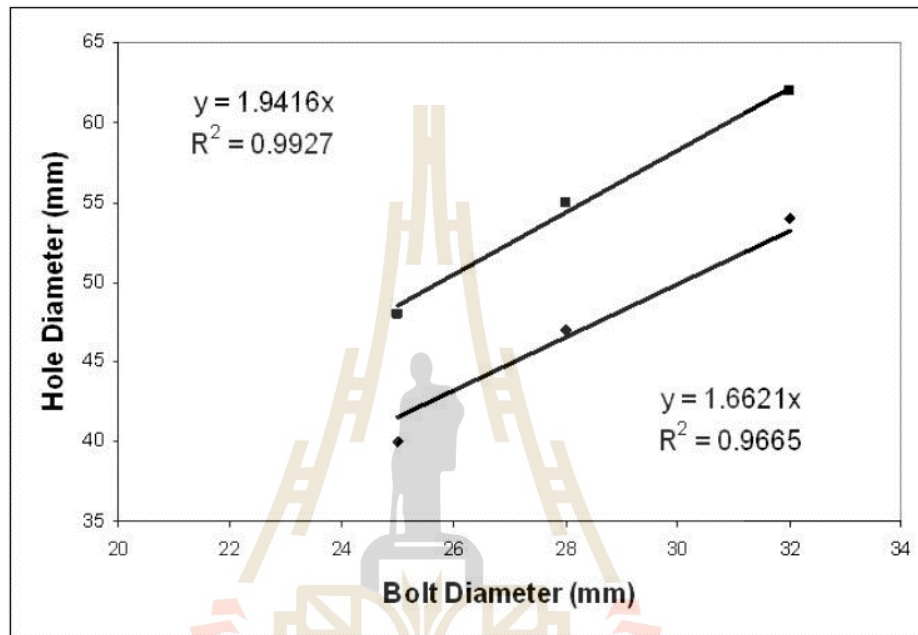


Figure 2.5 The optimal range between hole diameter and rock bolt diameter (Ghazvinian and Rashidi, 2010).

2.5.6 Size effect

Bazant and Sener (1988) investigated the size effect on the pull-out test by using cube specimens with cube sides $d = 38.1, 76.2,$ and 152.4 mm that were cast with deformed reinforcing bars. The steel bars are 2.9, 6.4 and 12.7 mm in diameter. The ratio of the mixer is water:cement:sand:gravel = 0.6:1:2:2. The squares are embedded by bolts length of 12.7, 25.4 and 50.8 mm and are then filled with epoxy. The results indicate two modes of failure; 1) The most splitting failures occurred in the medium and large specimens. The fractures are brittle and have an observation line crack. Spitting failure is much more progressive than shear failure of the fresh fracture mechanical type. 2) The shearing failures occurred in a small specimen. The fracturing has been characterized by plastic or less brittle lugs that shear or crush in front of the lug, which causes friction along the internal surface of

the cylinder. Pull-out maximum load from small specimen is more than medium and large specimen about 10 times and 3 times.

2.5.7 Bolt properties

Komurlu and Demir (2019) perform numerical modeling and laboratory testing to study the length effect on load bearing capacities of the split set type friction rock bolts. The results show that the load bearing capacity per one meter length is to be found decreasing with an increase in the length of the bolt shank from 1 m to 2.5 m on the three rock types (Chalcopyritic Ore, Limestone, and Dacite). In the experimental study, the load bearing capacity of bolts with a length of 2.5 m was greater than bolts with a length of 1 m. For numerical study, varied lengths from 1 m to 5 m have been found to decrease strength load per meter and increase strength load from higher lengths more than lower lengths, like in the experimental study at this 2.5 m rock bolt length. For equations from modeling that will be evaluated or useable in the same experimental test, whatever the load bearing capacity is not directly proportional to the length increasing.

2.5.8 Grout properties

Many researchers report that the mechanical properties of grouting materials have an influence on the capacity of rock bolts. The bolt bearing capacity increases with the increase in bolt length. Kilic et al. (2002) conduct pull-out tests on grouted rock bolts embedded into basalt blocks with cement mortar to evaluate the effect of grout properties on the bond strength of the bolt-grout interface of a treaded bar. The rock bolts with different diameters (10, 12, 14, 16, and 18 mm) and lengths (15.0, 25.7, 27.0, 30.0 and 32.0 cm) are bonded into the drilling hole (10 mm larger than the bolt diameter) in the basalt 16 blocks ($E = 27.0$ GPa and $\sigma_c = 133$ MPa). In order to obtain different grout types and different mechanical properties, grouting materials (10% sand, 5% fly ash, 10% fly ash and white cement within 21 days of curing time), curing time (1, 3, 5, 7, 14 and 21 days with $w/c = 0.4$), and water to cement ratio ($w/c = 0.34, 0.36, 0.38, \text{ and } 0.40$ within 21 days of curing time) are changed. The results indicate that the capacity of rock bolts depends on the mechanical properties of grouting materials. The bolt bearing capacity increases with the increase in bolt length and diameter by a constant thickness but it has a maximum load of the bolt shank limit is obviously decreased by the bolt bond strength. The mechanical properties of grouting materials can increase the bolt bearing capacity; the optimum water to cement ratio is 0.34-0.4. The increasing of

the bolt bearing capacity logarithmically is considered in the relationship between grout shear strength and bolt bond strength. Increased curing time increases the bond strength of the bolt rapidly in 1 to 7 days (19 kg/cm² to 77 kg/cm²) and slowly from 7 to 35 days (77 kg/cm² to 86 kg/cm²). Bond failure in the pull-out test is shear failure between the bolt and cement grout that characterized the shear spring from the evaluation of the ratio between bolt bond strength and grout shear strength. The ratio of both parameters is equal to or greater than 1, which means the bolt can bear capacity through grouting material, which causes failure on the grout-rock surface, while this result shows a value less than 1 that causes failure on the bolt-grout surface.

Portland cement grouted is a simple material between bolts and the interface of rock, thus, they investigate the ratio of water and cement (CEM II/B-P 32.5 R) mixture (w/c). The ratio of w/c is 0.34, 0.36, 0.38 and 0.40. The curing time of grout in basalt rock is 35 days. In general, bolt bond strength (τ_b) correlates with the maximum pull-out load of the bolt (P_b) followed by Littlejohn and Bruce (1975):

$$\tau_b = P_b / \pi d_b l_b \quad (2.2)$$

where d_b is bolt diameter; l_b is bolt length; $\pi d_b l_b$ is bond area. From testing, pull-out test of grout in high w/c ratio has been pull-out load of bolt higher than low w/c ratio, and then increasing the mechanical properties of material, as shown in Table 2.1. It observes that increasing shear strength and uniaxial compressive strength of grouting material increased bond strength of bolt, due to volume of water decreasing, as shown in Figure 2.6. Because of water is an admixture of cement that evaporation of excess water and construct porosity in the rock. The failure internal rock performs at rock bolt and grout material, greatly failure mode is shear at the bolt-grout interface (Hoek and Wood., 1988). Nevertheless, grout with water to cement has optimum dosages, that is explained and determined by using Marsh cone test (Yahia, 2011; Jayasree and Gettu, 2008; Roussel and Le Roy, 2005)

Table 2.1 The influence of the water to cement ratio on the bolt bond strength (Kilic et al, 2002).

W/C	UCS _g (MPa)	τ_g (MPa)	A _b (cm ²)	P _b (kN)	τ_b (MPa)
0.34	42.0	11.9	102	80.9	7.93
0.36	38.9	11.3	102	79.0	7.75
0.38	33.3	10.7	102	77.4	7.59
0.40	32.0	10.3	102	75.3	7.38

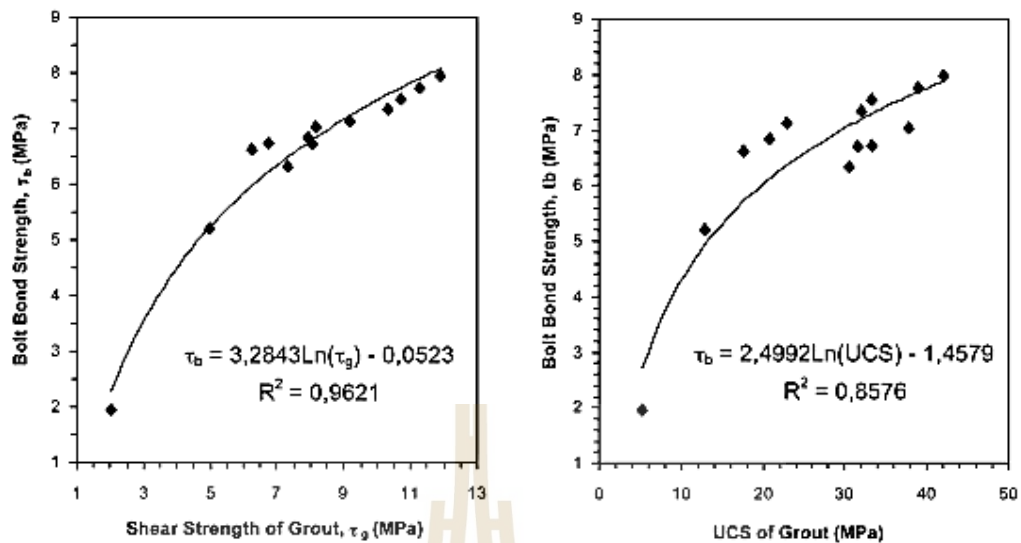


Figure 2.6 The relationship between grout of shear strength, uniaxial compressive strength, and bond strength (Kilic et al., 2002).

Normally, the mixer ratio of grout material is one effect that affecting to the force transmission. The load receiving and transferring of the molecule will good be distributed when the sample is close to homogeneous which depends on the type of material and optimal mixer ratio. Ji et al. (2011) find an effect of sand size and packing degree on flexural strength and compressive strength by using reactive powder concrete (RPC). The base materials are Grade 52.5 Portland cement, silica fume, and ultra-fine fly ash, which mix to produce different sand grades under the same weight ratio. The result shows that sample No. R2 has the highest strength of 195.0 MPa and flexural strength of 43.6 MPa when mixed with three sizes of diameter sand. The maximum grain size is 0.63 mm while sampling No. R4 has the largest grain size of every sample with a compressive strength of 163.9 MPa, but the amount of grain size is too many.

Zhang et al. (2020) research behavior and failure mechanisms by direct shear tests. In part of the grout mixture, the specimens comprise well-matched upper and lower sections that are made from cement (32.5R Portland) that has a cement-water ratio of 1:0.4 and differential cement-sand ratios (1:0, 1:1, 1:2). The result of shear stress of cubic specimens ($100 \times 100 \times 100 \text{ mm}^3$) under normal stresses of 0.25 MPa, 1 MPa, and 6 MPa shows a trend of shear stress and shear displacement curve to brittleness that compares to grout specimens without sand content. The shear stress and displacement increase with increasing cement-sand ratio and normal stress. The shear stresses of normal stress lower than 2 MPa have been values of cement-sand

ratio 1:2 more than cement-sand ratio 1:1 The displacement of cement sand-cement 1:2 more than cement-sand 1:1 until at normal stress 6 MPa, the ratio become alternately and the displacement of both ratios have the peaks less than lower normal stresses. The reduction of shear stiffness in sand content is smaller than the rapid reduction of specimens without sand.

Kang et al. (2013) study the densification of interfacial transition zone (ITZ) by using the pull-out test. The specimen comprises three types of fiber reinforcements in the mortar that have a diameter of about 0.3-0.4 mm. (Smooth fiber, Hooked fiber, and Twisted fiber). Materials for mortars are varied three grades of sand size and the ratio of sand to cement (s/c). The diameters of sand types SS40, SS60 and SS80 are 0.42, 0.22 and less than 0.2 mm in order. For compressive strength, there has been an increase in the value from 80 MPa to 90-102 MPa with decreasing of grain size while s/c = 1.5 for finer grain size has more influence and is more sensitive than s/c = 1.0 due to the larger surface area of fine sand and the higher concentration of Calcium Silica Hydration reaction in more than coarse sand. For single fiber pull-out shows maximum pullout stress of T-fiber in high s/c ratio and finer grain is more than S-fiber, which has frictional bond strength, but the pullout resistance is unclear in the characteristic of H-fiber because the pull-out load at high s/c ratio has not increased. Although two types of T and H fiber are the main mechanical interactions, T-fiber occurs along with embedment length, while H-fiber is the hooked end, which is building energy at the two plastic hinges. The image of backscattered electron (BSE) indicates grain size interface increase. Indentation for investigation is divided into 6 points (total = 60 micro-meter). At the first point (10 micro-meter) or nearest fiber reinforcing point, indentation hardness and modulus from calculated by loading period that focuses on the slop of unloading with constant maximum indentation load increase with finer grain sand by property of sand that is higher than the product of paste hydration or calcium silica hydrate, and then increase at the next point to be continuous. Displacement of period loading in high s/c ratio and finer grain size is always less than in low s/c ratio and coarse sand size.

2.5.9 Loading rate

Long et al. (2020) investigate the bond strength of steel reinforcement under different loading rates. Using various embedment lengths in testing (60 mm, 180 mm, 300 mm, and 420 mm), load rates start at a loading rate of 0.1 mm/s, 1.0 mm/s, 10 mm/s, and 100 mm/s by denoted LS, S, MS, and FS respectively. The level of load capacity involves absorption energy (Hao et al., 2020). Attention is drawn to the

embedment length of 60 mm. The samples LS-12-5 increase peak load values and steeply fail to reduce the residual force of the load-slip curve, which is the same result as Eligehausen et al. (1982). MS-12-5 has a peak value greater than LS-12-5 by the value of maximum bond stress 18.8 MPa, increasing to 22.6 MPa, or around 20%. Increasing the loading rate from 10 mm/s to 100 mm/s. Maximum bond stress decreases 20.8 MPa by 8% but is still more than loading 0.1 mm/s by 11% affecting residual bond stress. For embedment lengths of 180, 300, and 420 mm, maximum load increases as expected, but residual loads load more than peak force and 60 mm embedment length. As expected, an increasing load and rapidly distributed internal radial crack cannot fully propagate stress while shear strength increasing, peak shear strength occurs at higher shear displacement (Moosavi and Bawden, 2003). The normalize of maximum and residual bond stress is calculated by $22.46\sqrt{f_c}$ and $0.91\sqrt{f_c}$ by Eligehausen et al., in which f_c is the cylinder compressive strength. The sample LS-12-5 has a value of maximum and residual bond stress higher than normalized of maximum and residual stress bond around 46% and 71%. From all above, the strain rate distributed at the load end of reinforcement increasing is $2.9 \times 10^{-2} \text{ s}^{-1}$ by 17%. Along embedment will spread bond stress by dynamic loading (Takeda, 1984). Locality failure of all specimen occur when load is not reached yield strength of bolt (2,650 micro-strain), investigation of all embedment slip shows failure when ratio of strain at load end to yield strain of the reinforcement less than 1 in the namely of numerical of legend. So, embedment length more than 5 times and less than 15 times of diameter bolt is enough for bearing capacity in a bolt although failure remains fail at elastic phase.

Boshoff et al. (2009) explore the mechanical behavior of the single fiber pull-out under different loading rates. In the part of grout, there is a water/binder ratio of 0.4 and an aggregate/binder ratio of 0.5, with a curing time of 14 days. The results indicate that the effect of the pulling rate is 0.01, 0.1, 1, 10, and 100 mm/s. The first peak interfacial shear stress increases when loading rate increases, followed by an increase in the magnitude of frictional shear traction of about 91% similar to Maalej et al. (2005) and Boshoff and Van Zijl (2007). Characteristics of each loading rate carried out by pull-out load and displacement curve that show chemical bonds calculated from load drop after maximum load. At the highest rate, the damage to the fibre-matrix has 80% of fibre rupture that opposition with Yang and Li (2006) report that the cause may be from embedment less than half and same the report of Douglas and Billington (2005) which decreasing in tensile strain capacity with an increase of strain

rate. In the same way, single fiber can resist pulling that steady interfacial bond since strain rate 0.1 mm/s with completed pull-out failure and there is percent fiber rupture to low as strain rate 0.01 mm/s, while failure of faster rates (1 to 100 mm/s) form around single fiber from parameter investigated by increasing of slip-hardening/softening coefficient and SEM photo which appear edges of end fibers are cut.

Nieuwoudt and Boshoff (2017) determine the mechanical pull-out behavior of hooked-end and straight fibers. Embedment length and diameter of fiber are 15 mm and 0.9 mm, and the pull-out rate is varied from 2.5×10^{-4} mm/s to 2.5 mm/s, respectively. The results indicate load-slip curves of straight fibers have an immediate drop after the peak load is reached, friction is the main restraint between fiber roughness and the internal surrounding surface of the specimen, which is different from hooked-end fibers in that there is no abrupt decrease in load, which is similar to what was found by Cunha et al. (2010), while load drop after the peak is caused by the structure of hook-end fibers, which causes a foldable joint to stretch until 4.5 mm before going into the residual phase. Summary of ultimate force and slip at ultimate force, straight fibers have values of $P = 0.957 > 0.05$ and $P = 0.753 > 0.05$, while hooked-end fibers have values of $P = 0.0198 < 0.05$, which indicates the behavior of hooked-end not straightening completely. However, there was a significant effect on pulling rate with $P = 0.425 > 0.05$, as shown by Joo Kim (2009).

Zhao et al. (2015) study and simulate pull-out test with 200 mm anchor embedment length by particle flow code software (PFC2D). The specimen size is $300 \times 300 \text{ mm}^2$. The differential loading rates from 0.5 mm/s to 1000 mm/s are used in this test. The result shows load – displacement curve divided in three groups with soft scop (loading rate $< 10 \text{ mm/s}$), moderate scop ($10 \text{ mm/s} < \text{loading rate} < 100 \text{ mm/s}$) and strong scop (loading rate $> 100 \text{ mm/s}$) that give the load with less than 60 kN, 60 – 90 kN, and more than 100 – 300 kN as the displacement implicated to rapid drop shear stress after failure. In part of axial force interesting to the distribution force to along a bolt. Especially, the high rates provide the higher axial force where the load is close to the load end more than the lower rates but after middle section of the bolt cannot bear the load as the lower rates until the end of the bolt from matrix particle with radius 1.3 – 1.7 mm which concentration is developed stress in upper and middle bolt section.

2.6 Energy absorption

For finding energy in a fully grouted rock bolt that comes from bearing capacity in the bolt. The area under the load-displacement curve is the total energy measured

from the load end. So, the capacity and length of a bolt are the main factors in keeping energy in the individual test. Hao et al. (2020) study increasing loading capacity by adding equipment for reinforcement. The diameter and number of steel balls are varied in this testing with constant support of about 290 - 300 mm. The result of amount of steel balls shows that with a 4 mm diameter constant that increasing from 4 to 9 makes constant working resistance increase from 60 to 120 kN in batch 1, while constant working resistance in batch 1 is increased from 87 to 136 kN by the number of steel balls, which is 9 pieces with an increasing diameter between 3.5 and 4.5 mm. After load-displacement curves are shown, the areas are also identically indicated too. Energy-absorbing capacity in batch 1 increased from 58.87 to 110.37 kJ/m while in batch 2, it increased from 66.68 to 123.28 kJ/m. Although the stiffness of 8 pieces and the largest diameter (3 mm) of steel balls start steady at the highest values of 3.56 and 4.00 kN/mm. Immortal stiffness is observed with the slope of the supporting load and roof to floor convergence that prevent major rock failure, as shown in Figure 2.7. In part, this loading rate of with 0.1-20 kN/min relates to the velocities of the experimentation by Ansell (2006) that the initial load is 400 and 450 MPa. This reason that dynamic loads are supported more than static loads with loads of 440 MPa in this absorption energy of rock bolts.

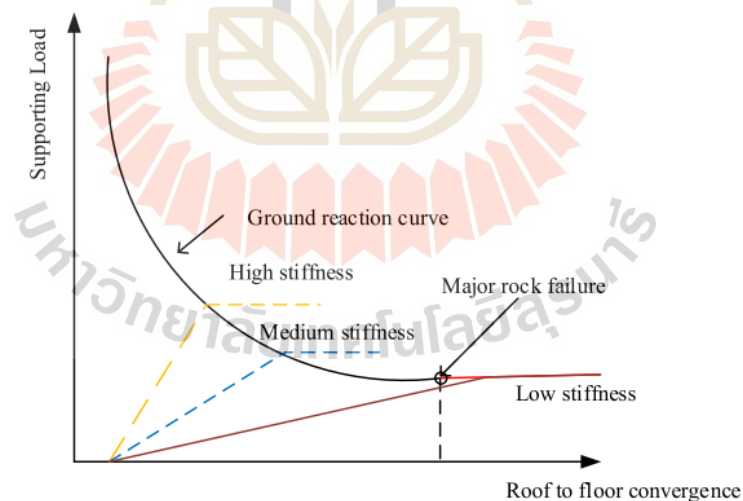


Figure 2.7 Bearing capacity in the ground reaction curve (Hao et al, 2020).

Dai et al. (2018) design the new energy absorber for supporting the dynamic load in the roadway that shows in terms of energy daily and displacement about 2 mounts with micro-seismicity in Figure 2.8. The absorbers are varied in angles, thicknesses, and diameters. The result indicated an important role of thickness in that the angle of 30 degrees gives the maximum load, and the constant load has been

more than 45 degrees in each diameter (26 and 28 mm). The thickness of less than 4 mm has low peak values, although the diameter of the absorber is the largest (28 mm). So appropriate diameter and thickness are 26 mm and 4 mm with 30 angle degrees, which is the full performance of the axial component's absorbed total energy (13.06 - 14.61 kJ) in this testing by without peak load or showing in the plateau load at the initial displacement until the test end. The stoke efficiency (SE) of the absorber is in the part of quality steel material that leads to 88.67% by adding 2 mm thickness. In part of economics, total cost is from retrofit (QR) plus addition cost (QA) which costs about 20-50 yuan and does not exceed 57 yuan for a new single-absorbing bolt. This can be examined following Tahmasebinia et al. (2018), Wu et al. (2018) and Li (2011) with numerical simulation for estimation of shear load and shear displacement, including equation analysis components by six parameters in the FLAC3D software, and complying with any bolt type for burst prevention and reducing cost in the process.

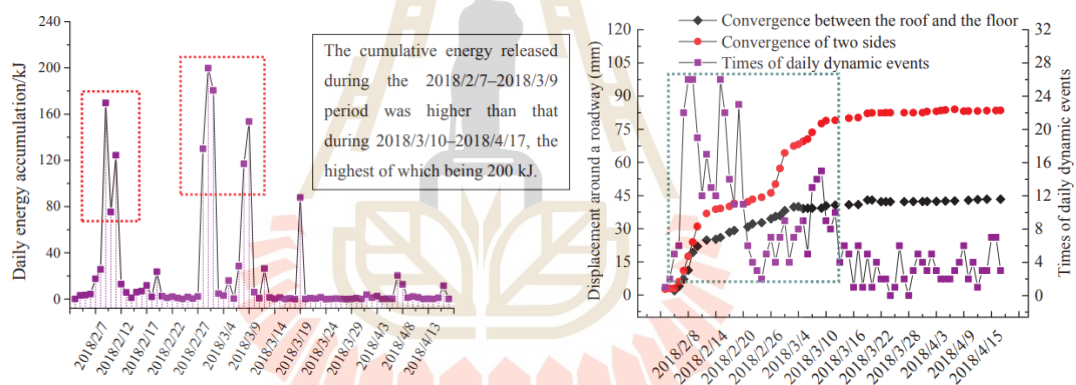


Figure 2.8 Deformation curve of moving and energy daily absorption in the roadway by measuring micro seismic wave (Dai et al, 2018).

Li (2010) compares capability anchor bolt types with resin and cement for static and dynamic pull-out tests. Types of anchors divide into two forms, paddle-anchored and wiggle-anchored, in which both bolts remain D-bolts with 20 - 22 and 17.5 -20 mm diameters, respectively. After test static load, the result of different diameters of both bolts increases load with the larger diameter, though ultimate strain is the same, while part of material grout shows pull-out load coated with shrink pipe, which has no or little effect due to the higher maximum strain (20%), while cement has little value less than resin but replacement with more than displacement in the same diameter by maximum strains of 18% and 20% in resin and cement grout (42 and 48 mm), and all of paddle-anchored fail with necking stretch about 10 mm as Figure 2.9. In part of dynamic load, mass load is dropped to add weight (total weight = 893 kg) and

calculated in terms of energy by the average cumulative energy of approximately 38 kJ in bolt length of 0.795 m, or 47 kJ/m, and there is maximum strain of about 15 - 20% correspond to static loading.



Figure 2.9 Sample of Paddle – anchor during testing until after testing (Li, 2010).



CHAPTER 3

SAMPLE PREPARATION

3.1 Introduction

This chapter describes the basic material used in the testing. Materials used in this experiment are natural sand, Portland cement, sandstone samples and rock bolt.

3.2 Natural sand

The natural clean sand used in the content of cement grout is a basic material. The chemical properties of sand have the molecule bond of silica dioxide stronger than the product of hydration reaction, therefore sand can help increase strength with optimum ratio. Normally, sand size will give differential compressive strength. In this study, tester used sand sizes less than 0.85 mm but more than 0.425 mm by using sieves number 20 and 40 as shown in Figure 3.1. Quantity of sand that appropriately adjusted with experimental testing. The ratio of sand to cement is 1:1 by weight.



Figure 3.1 Sieve size number 20 and 40 sorted natural sand.

3.3 Portland cement

Portland cement type 1 is used and it is guaranteed by ASTM C150 standard practice that this type is always used in common building foundations, beams, and work for bearing capacity. The cement bag containing 50 kg, is from the Siam City Cement Public Company Limited, Thailand. The cement bag prevents cement from humidity in cool-dry areas (Figure 3.2). The properties of Portland cement conform to SCCC, which is autoclave expansion of 0.006%, initial setting time of 118 minutes, and final setting time of 215 minutes. The air content in mortar is 10%. The compressive strength for 7 and 28 days is 37 and 45 MPa, respectively. Regularly, cement will mix with sand, gravel, or rock according to usability and the objective user.

In this preparation, the cement grout is mixed with the cement, sand, and freshwater by the mechanical mixing (Figure 3.3). The ratio of water to cement and cement to sand is 0.45:1, and 1:1. The mixing procedure starts from:

- The first step is to mix water into the bowl and gradually fill it with cement by stirring the paddle at low speed (140 ± 5 r/min) for 30 seconds.
- Next is add sand slowly over a 30-s period and then change speed to medium speed (285 ± 10 r/min), and mix for 180 seconds.
- During mixing, always scrape any mortar that has been collected on the side into the batch.
- Mixing until complete the time with a total time about of 5 minutes.

The complete mixture is poured into the polyvinyl chloride tube (PVC). The PVC molds are cut with a length of 108 mm and a diameter of 54 mm. The PVC mold which is polished with sandpaper until smooth is attached by resin on the acrylic plate (Figure 3.4). The cement grout in a PVC tube is cured in the water at room temperature for curing times of 3, 7, 14, 21, and 28 days. The cement specimens are cut out of PVC tubes with a L/D as 2.0 for the uniaxial compression test. In another part, the cement is grouted into the hole of the sandstone specimen and cured in water for a period time of 7, 14, 21, and 28 days for pull-out tests. Table 3.1 summarizes the basic parameters of cement grout specimens (specimen number, length, diameter, weight, ratio of length/diameter, and density).



Figure 3.2 Portland Cement Type 1 is used in this study.



Figure 3.3 Mixer, Kitchenaid Professional 600 6QT 575 watts stand mixer, with maximum capacity of 5,000 cc and 6 speed control.

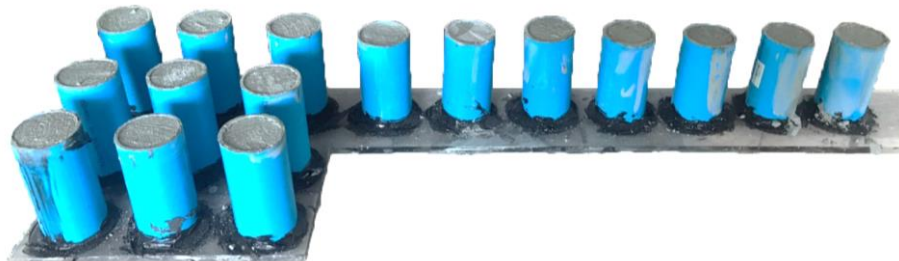


Figure 3.4 Casing grout specimen in PVC tube for compression test.

Table 3.1 List of specimen number, length, diameter, weight, ratio of length/diameter and density.

Sample No.	Rock Type	D (mm)	L (mm)	W (g)	L/D	ρ (g/cc)
3CS-1	Mortar	55.0	110.7	549.9	2.0	2.09
3CS-2	Mortar	55.0	110.7	551.2	2.0	2.10
3CS-3	Mortar	55.1	108.3	537.2	2.0	2.08
3CS-4	Mortar	54.5	112.9	557.8	2.1	2.12
3CS-5	Mortar	54.2	112.8	561.8	2.1	2.15
3CS-6	Mortar	54.8	112.5	563.4	2.1	2.12
7CS-1	Mortar	54.3	109.8	547.2	2.0	2.15
7CS-2	Mortar	54.6	111.8	555.8	2.0	2.12
7CS-3	Mortar	54.8	111.0	558.7	2.0	2.13
7CS-4	Mortar	54.3	111.9	561.4	2.1	2.17
7CS-5	Mortar	54.4	110.6	550.2	2.0	2.14
7CS-6	Mortar	54.7	111.7	552.5	2.0	2.10
14CS-1	Mortar	54.9	110.6	554.2	2.0	2.11
14CS-2	Mortar	54.8	111.5	559.8	2.0	2.13
14CS-3	Mortar	55.2	110.8	554.7	2.0	2.09
14CS-4	Mortar	54.4	107.0	537.4	2.0	2.16
14CS-5	Mortar	54.2	107.4	528.7	2.0	2.13
14CS-6	Mortar	54.2	108.1	545.7	2.0	2.19
21CS-1	Mortar	55.2	111.9	561.6	2.0	2.10
21CS-2	Mortar	54.2	110.5	553.4	2.0	2.17
21CS-3	Mortar	54.8	112.5	559.7	2.1	2.11
21CS-4	Mortar	54.2	113.3	567.9	2.1	2.17
21CS-5	Mortar	54.6	108.5	540.5	2.0	2.12
21CS-6	Mortar	54.9	111.6	558.7	2.0	2.11
28CS-1	Mortar	54.7	112.3	555.7	2.1	2.11
28CS-2	Mortar	54.8	111.4	555.7	2.0	2.12
28CS-3	Mortar	54.9	112.4	565.3	2.0	2.12
28CS-4	Mortar	54.4	116.5	585.0	2.1	2.16
28CS-5	Mortar	54.1	113.8	566.6	2.1	2.16
28CS-6	Mortar	54.5	112.5	559.3	2.1	2.13
28CS-7	Mortar	54.8	108.6	544.9	2.0	2.13

3.4 Sandstone sample and rock bolt

The sandstone rock samples are carried out as shown in Figure 3.5 by cutting with dimensions $110 \times 110 \times 200 \text{ mm}^3$ (width \times length \times height) at Suranaree University of Technology for pull-out testing. The qualities of Phra Wihan sandstone are collected in terms of mechanical properties. There are uniaxial compressive and tensile strengths of 54 MPa and 6.7 MPa, respectively. The elastic and Poisson's ratios are 10.8 GPa and 0.23, respectively. The cohesion and internal friction angles have values of 3.1 MPa and 46 degrees, respectively (Fuenkajorn and Kenkhunthod, 2010; Kapang et al., 2013; Phueakphum et al., 2013). The hole of rock block is drilled through with a smooth surface of 25 mm diameter by using a driller. The bolt is 12 mm in diameter and threaded on the top end (Figure 3.6). The heater bypass cap (Figure 3.7) drilled hole is stuffed with bolts for setting on a vertical line in the center hole and plugged with cement to prevent flow out. The type of heater bypass cap is nitrile rubber that can withstand oil and fire to protect against the heat of hydration and the chemical reaction of cement and water. The cement plug is a 100 mm embedment in the top hole of the sandstone specimen. The specimens are cured in the water for 7 to 28 days before the pull-out test. Table 3.2 summarizes the specimens' number, grout type, diameter bolt, diameter hole, embedment length, and ratio of length/diameter of the tested specimens.

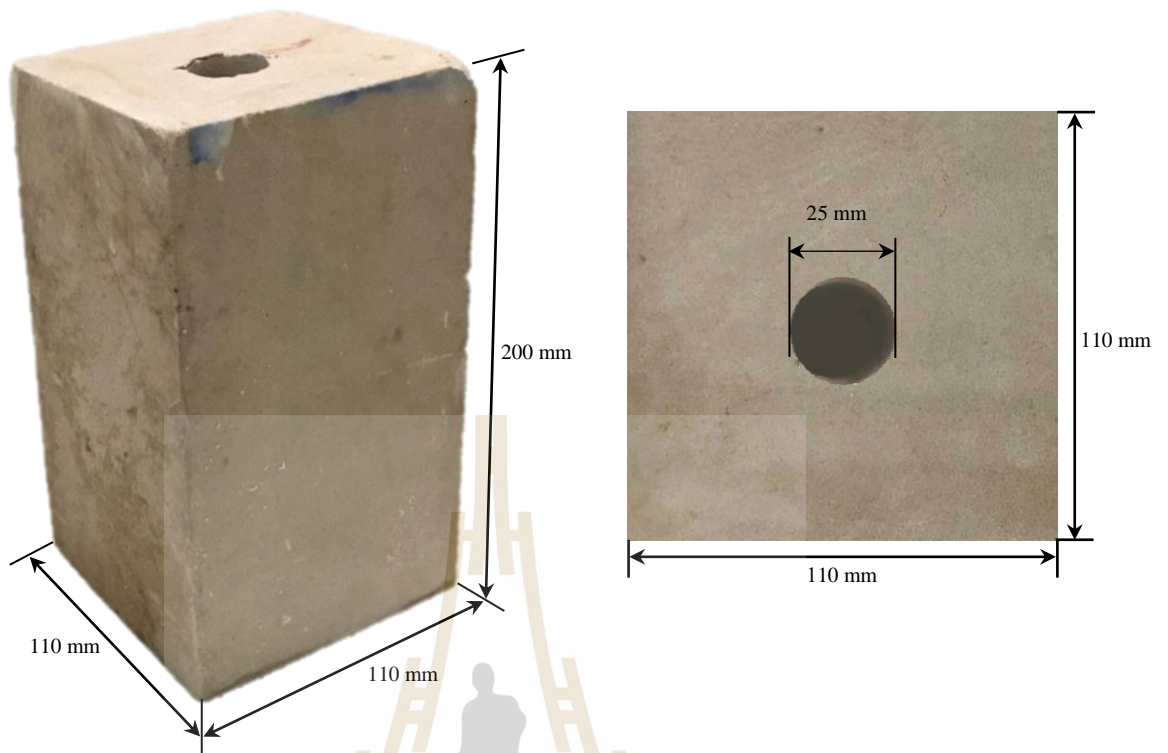


Figure 3.5 Sandstone specimen with dimension $110 \times 110 \times 200 \text{ mm}^3$ by saw cut surface and drilled with 25 mm diameter hole.



Figure 3.6 Deformed bar with 12 mm diameter for pull-out test.



Figure 3.7 Heater bypass cap for plugging grouting material.

Table 3.2 List of number specimen, grout type, diameter bolt, diameter hole, embedment length, and ratio of embedment length/diameter.

Sample No.	D_{Bolt} (mm)	D_{Hole} (mm)	L (mm)	L/D (mm)
7LR1-1	12.00	25.25	100.00	3.96
7LR2-1	12.00	25.62	100.00	3.90
7LR3-1	12.00	25.50	100.00	3.92
7LR4-1	12.00	25.85	100.00	3.87
14LR1-1	12.00	25.95	100.00	3.85
14LR2-1	12.00	25.75	100.00	3.88
14LR3-1	12.00	26.00	100.00	3.85
14LR4-1	12.00	25.35	100.00	3.94
21LR1-1	12.00	25.65	100.00	3.90
21LR2-1	12.00	25.85	100.00	3.87
21LR3-1	12.00	25.68	100.00	3.89
21LR4-1	12.00	25.90	100.00	3.86
28LR1-1	12.00	25.40	100.00	3.94
28LR2-1	12.00	25.55	100.00	3.91
28LR3-1	12.00	25.95	100.00	3.85
28LR4-1	12.00	25.10	100.00	3.98

CHAPTER 4

LABORATORY TESTING

4.1 Introduction

This chapter presents the test methodology and test results. The laboratory experiment performed here can be divided into two main types: (1) the uniaxial compression test on cement grout and (2) the pull-out test on bolts reinforcement system. The results are used to determine the performance of bolts reinforcement system under the difference loading rate and curing time. Moreover, they can be used to formulate the mathematical relation between pull-out load, loading rate, and curing time which is presented in the next chapter.

4.2 Uniaxial compression test

The objective of this test is to determine the uniaxial compressive strength, Poisson's ratio, and elastic moduli of grouting material. The tests are performed on cylindrical specimens with a nominal diameter (D) of 54 mm and length (L) of 108 mm (L/D ratio = 2.0) as shown in Figure 4.1. The cement grout specimens are cured in PVC molds for 3, 7, 14, 21, and 28 days before testing. The tests are performed by increasing the axial stress until failure occurs with loading rate of 1 MPa/s (ASTM 7012-14). The axial and lateral displacements are monitored by using dial gages (Figure 4.2). The compressive strength (σ_c) is determined from the maximum load (P_{max}) divided by the original cross-section area (A):

$$\sigma_c = \frac{P_{max}}{A} \quad (4.1)$$

The uniaxial compressive strength, elastic modulus, and Poisson's ratio of grouting material are summarized in Table 4.1. The results indicated that the uniaxial compressive strengths increase, and Poisson's ratios decrease when curing time as shown in Figures 4.3 through 4.4. The compressive strength is increased by 35% when the curing time is increased from 3 to 28 days while elastic modulus is independent of curing times (Figure 4.5). Figure 4.6 shows the post-test specimens and failure pattern. Fracture occurs parallel and along the loading direction.

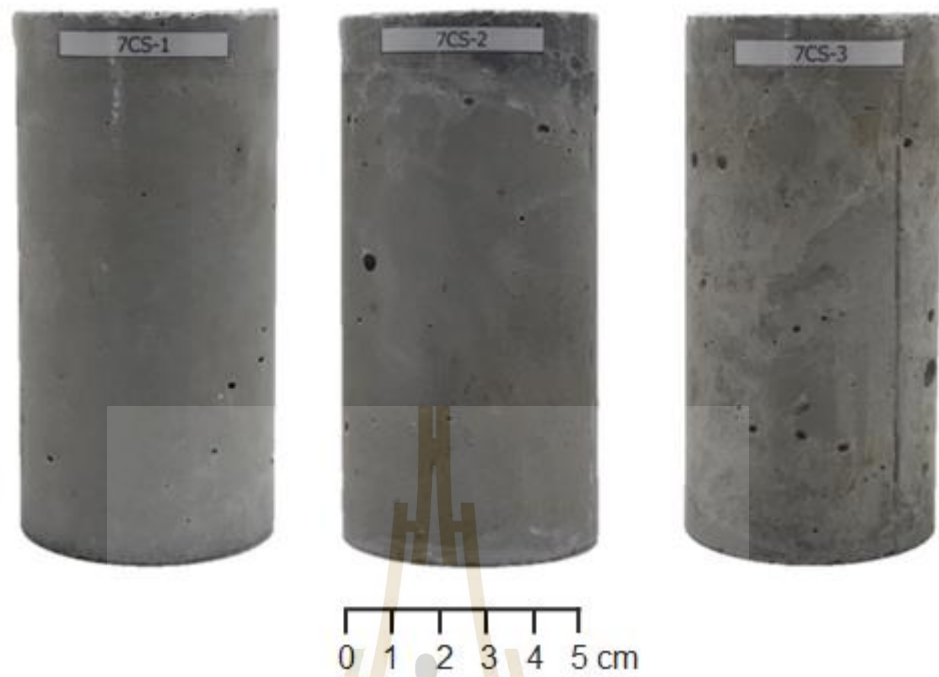


Figure 4.1 Some grouting specimens with ratio of $L/D = 2.0$ prepared for uniaxial compression test.

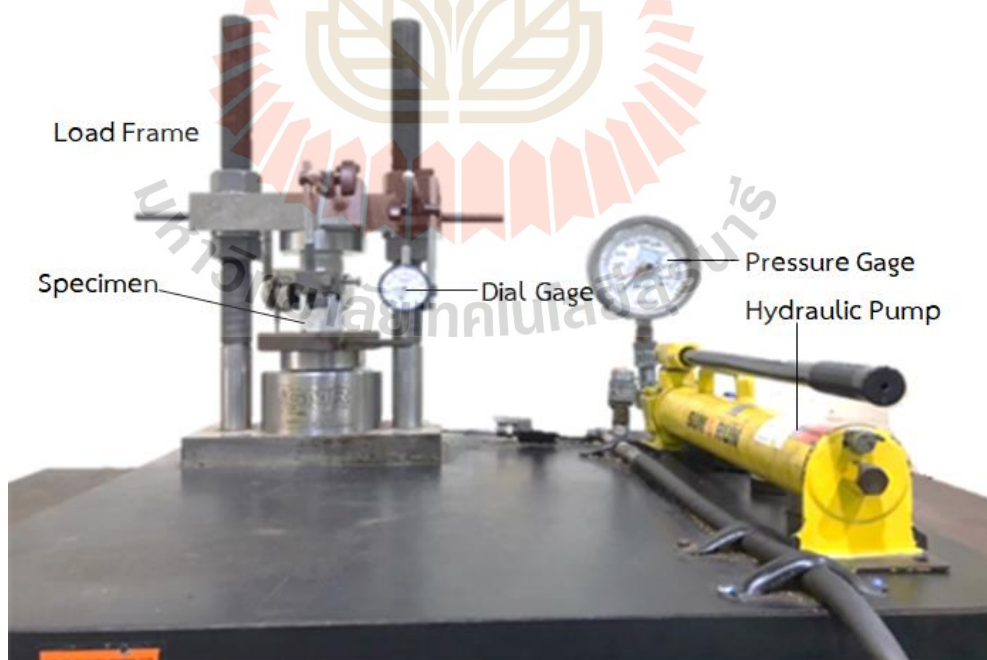


Figure 4.2 Test arrangement and apparatus for the uniaxial compressive strength test on the cylindrical shape cement-grout specimen.

Table 4.1 Uniaxial compressive strength (σ_c), elastic modulus, and Poisson ratio of cement grouting in the curing time function.

Sample No.	Curing Time (Days)	σ_c (MPa)	E (GPa)	ν
3CS-1	3	25.3	11.0	0.24
3CS-2		29.5	7.5	0.24
3CS-3		25.2	5.9	0.25
3CS-4		27.9	4.8	0.26
3CS-5		23.8	7.5	0.25
3CS-6		25.5	5.5	0.24
Average		26.2±2.0	7.0±2.1	0.25
7CS-1	7	34.6	7.0	0.23
7CS-2		29.9	7.1	0.23
7CS-3		29.7	6.1	0.22
7CS-4		36.7	7.4	0.23
7CS-5		32.3	8.4	0.22
7CS-6		29.8	6.3	0.23
Average		32.2±2.3	6.7±0.4	0.23
14CS-1	14	38.0	6.1	0.22
14CS-2		33.9	6.2	0.22
14CS-3		33.5	6.6	0.22
14CS-4		34.4	6.6	0.23
14CS-5		32.5	4.4	0.22
14CS-6		39.1	7.8	0.22
Average		35.2±2.0	6.3±0.2	0.22
21CS-1	21	41.8	8.0	0.20
21CS-2		36.9	7.6	0.21
21CS-3		38.2	6.0	0.21
21CS-4		36.8	4.4	0.21
21CS-5		34.1	4.8	0.20
21CS-6		35.9	6.3	0.20
Average		37.3±2.1	7.2±0.9	0.21
28CS-1	28	38.3	8.4	0.18
28CS-2		38.2	6.8	0.19
28CS-3		42.2	6.5	0.19
28CS-4		36.6	7.2	0.19
28CS-5		45.7	8.3	0.18
28CS-6		47.2	8.1	0.17
28CS-7		36.1	7.1	0.19
Average		40.6±1.9	7.2±0.8	0.18

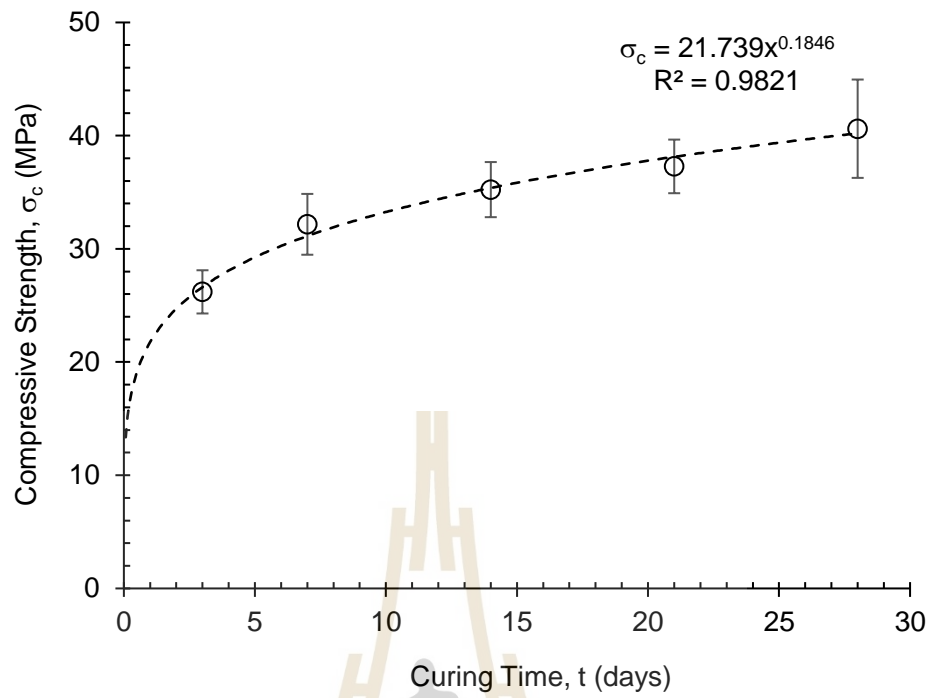


Figure 4.3 Uniaxial compressive strengths as a function of curing times.

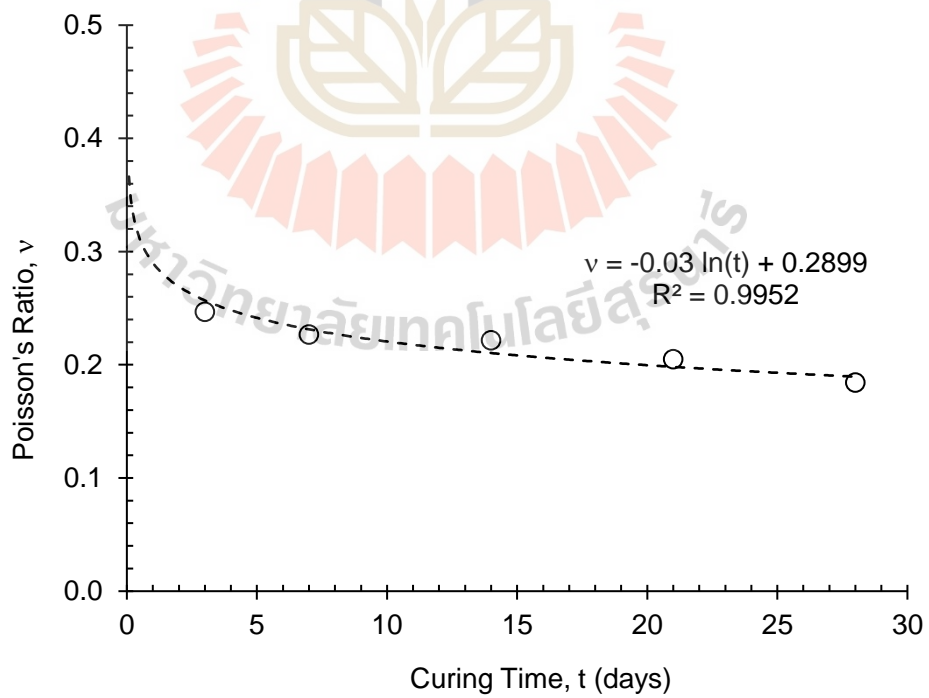


Figure 4.4 Poisson's ratio as a function of curing times.

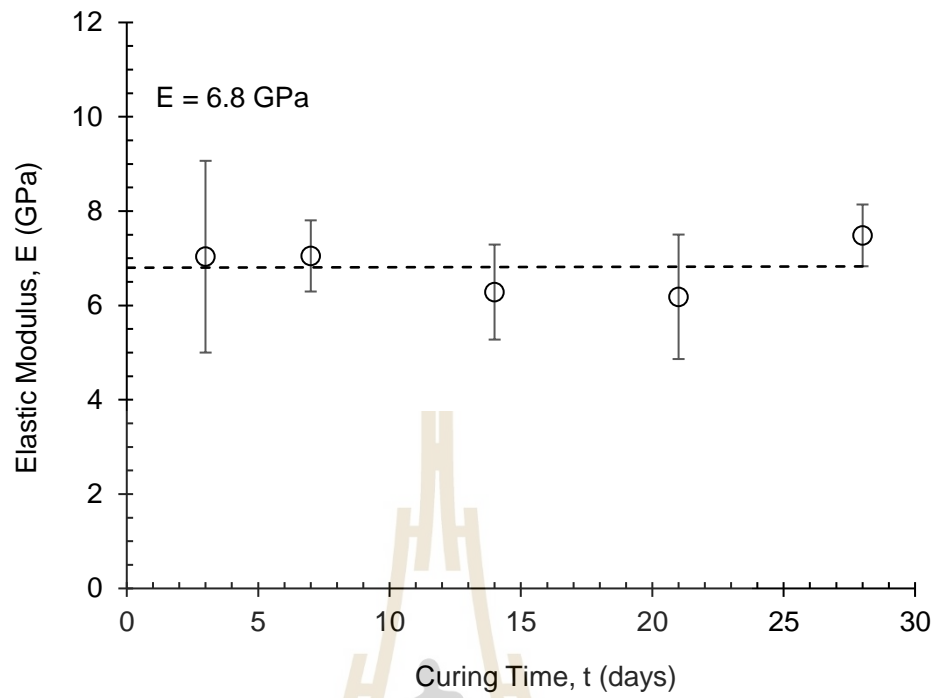


Figure 4.5 Elastic modulus as a function of curing times.



Figure 4.6 Some post-test specimens were obtained from the uniaxial compression test on the cement-grout sample when cured for 3, 7, 14, 21, and 28 days.

4.3 Pull-out test

The aim of this laboratory test is to determine the maximum pull-out load of the bolts reinforcement system under various curing time and loading rates. The test procedure follows the ASTM D4435-13E1 standard practice. The pull-out tests are conducted on the samples where cement grouts are cured at 7, 14, 21, and 28 days under loading rates of 0.1, 0.01, 0.001, and 0.0001 mm/sec, respectively. The grouting materials are cast in a hole at the center of the rock specimen with a diameter of 25 mm and length 100 mm. The rock specimens used here are obtained from Phra Wihan sandstone. They were cut by cutting machine to obtain the nominal dimension of $110 \times 110 \times 200 \text{ mm}^3$ (Figure 4.7). Figure 4.8 shows the hydraulic pump is placed on the top of rock specimen and exert pulling force to the nut on a 12 mm rock bolt.

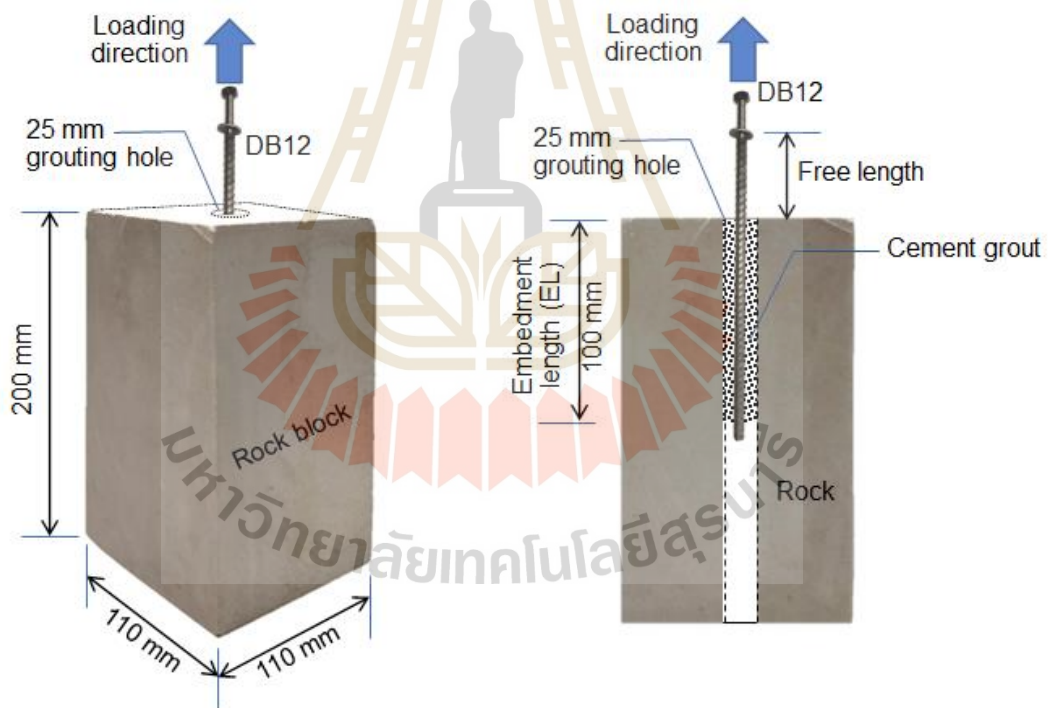


Figure 4.7 Sample preparation for pull-out test.

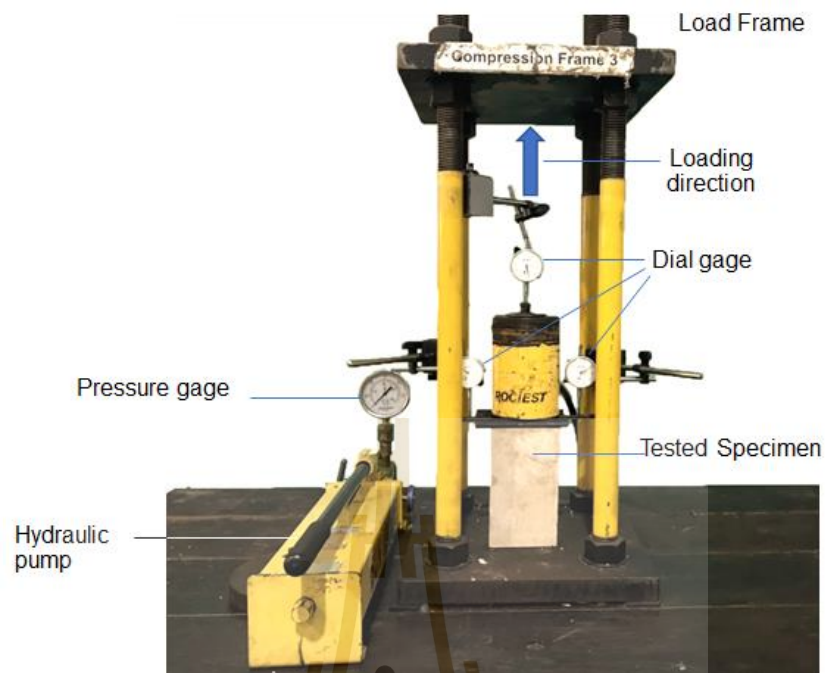


Figure 4.8 Pull-out test apparatus and test set up for pull-out test.

The pull-out load and displacement are plotted in Figure 4.9. The cross symbols (x) represent the peak pull-out load obtained for each curing time and loading rate. For the same curing time, the test under highest loading rate (0.1 mm/s) gives a higher peak load than those under lowest loading rate (0.0001 mm/s). Table 4.2 summaries of the peak load and maximum displacement where failure occurred. The relationship between curing time and peak load under various loading rates is plotted in Figure 10. Moreover, the curing time is plotted as a function of the maximum displacement under different loading rates (Figure 11). The displacement measured from pull-out increased with the increasing of curing time and decreased with the decreasing of loading rate. Figures 12 through 15 show the post-test specimens with many modes of failure under the different loading rate of 7, 14, 21, and 28 days, respectively.

Figure 4.16 shows the classification of failure modes that can occur during the pull-out test. Based on the 7 failure modes proposed by Ren et al. (2010): (a) in the rock bolt, (b) in the grouting material, (c) in the rock block (representing the rock mass), (d) at the bolt-grout interface, (e) at the grout-rock interface, and (f) a combination of these failure modes. The cone-shaped shear zone develops near the outer boundary of rock block can be obtained for all test conditions. The higher compressive stresses and deeper distribution in the compression zone at the outer surface of the rock block can be obtained for sample when it was tested under a low pull-out rate on longer

curing time. As a result, the pull-out test under low pull-out rate (0.0001 mm/sec) for high strength of grout material (curing 28 days) yield wider and deeper conical shear zone than those obtained under a high pull-out rate (0.1 mm/s) on low strength of grout material (curing 7 days). Table 4.3 summarizes the failure modes observed on the post-test specimens. The patterns of failure modes are divided into two groups: In rock bolt-grouting material that occurred in the first or second weeks and combined failures mode with broken grouting material because the strength of grouting material is not enough to bear capacity of pull-out load and following debonded interface between rock bolt and grouting material, along with Poisson's ratio of grouting material more than rock sample, therefore, resulting in broken of rock block until to 14 days. Uniaxial compressive strength of grouting material reaches 35 MPa or more than 80% of uniaxial compressive strength at cured 28 days, it can bear a capacity of pull-out load which a loading rate less than normal loading rate or a curing time of more than 14 days but the interface of grout-rock has less shear strength than the interface of bolt-grout and thus, the failure mode is formed with debonding between grout-rock interface and appearing obvious core of cement plug.

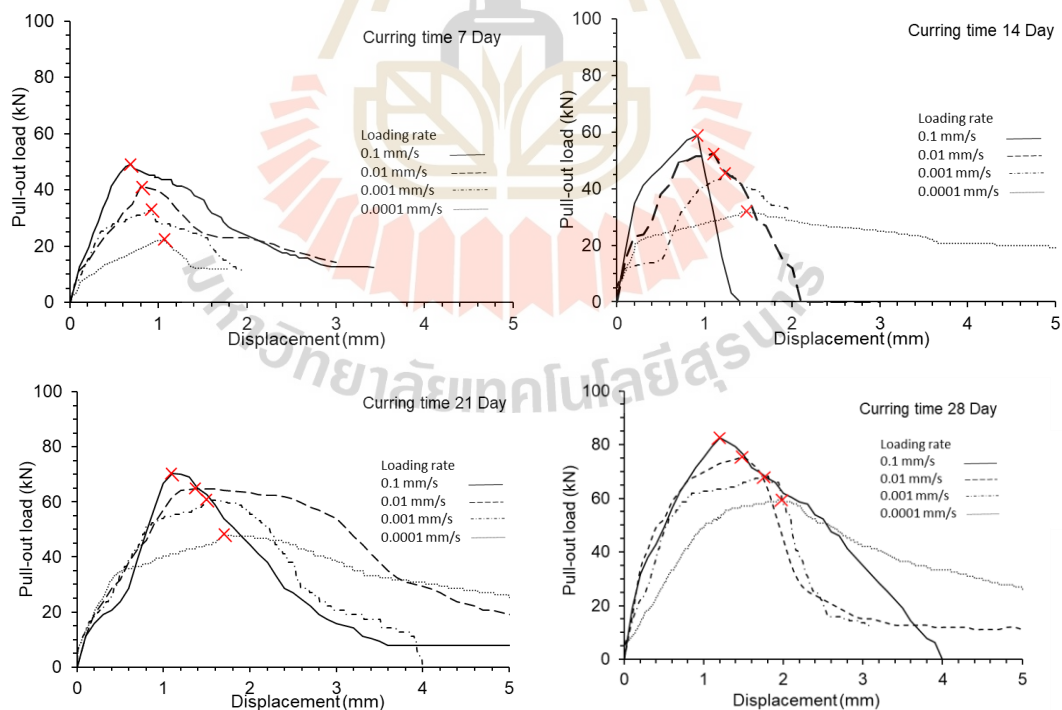


Figure 4.9 Load-displacement curve obtained for 7, 14, 21, and 28 days of curing samples under various loading rates. The cross symbols represent the ultimate pull-out load for such loading rate.

Table 4.2 Test results under different loading rates with pull-load and maximum displacement as a function of curing time.

Sample No.	Curing Time (days)	Loading Rate (mm/sec)	Pull-out Load (kN)	Maximum displacement at failure (mm)
7LR1-1	7	0.1	49.17	0.68
7LR2-1		0.01	41.20	0.80
7LR3-1		0.001	33.31	0.92
7LR4-1		0.0001	22.37	1.06
14LR1-1	14	0.1	58.95	0.92
14LR2-1		0.01	52.34	1.10
14LR3-1		0.001	45.54	1.23
14LR4-1		0.0001	31.72	1.43
21LR1-1	21	0.1	70.20	1.10
21LR2-1		0.01	64.80	1.35
21LR3-1		0.001	60.80	1.50
21LR4-1		0.0001	47.80	1.68
28LR1-1	28	0.1	82.48	1.20
28LR2-1		0.01	75.20	1.50
28LR3-1		0.001	68.21	1.72
28LR4-1		0.0001	59.48	1.94

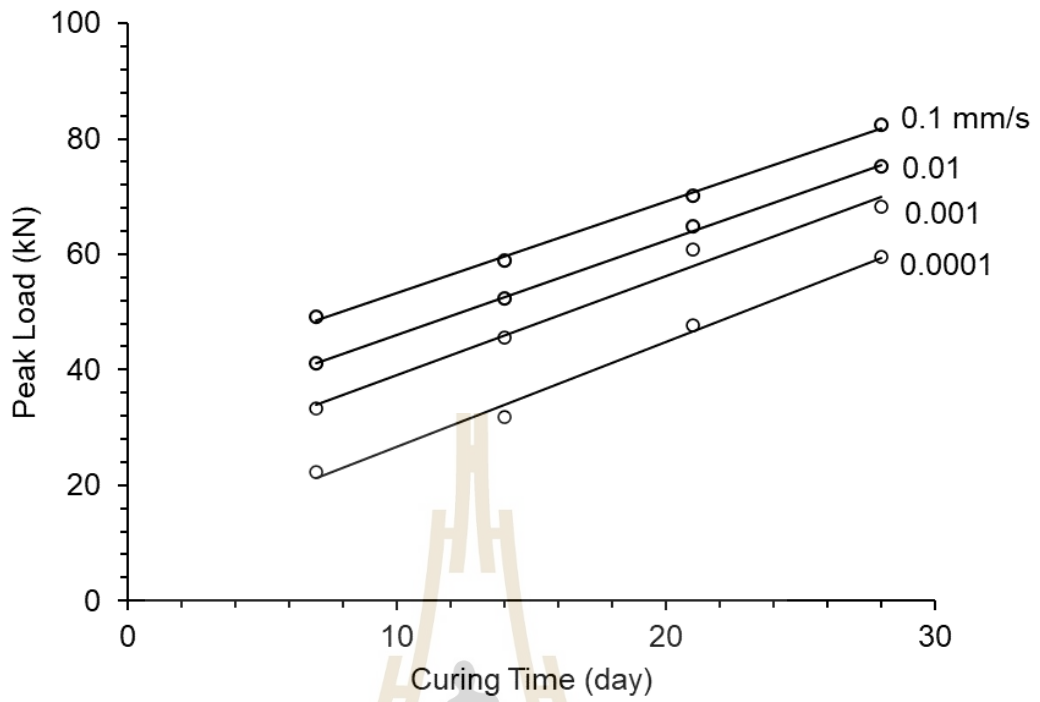


Figure 4.10 Peak load of pull-out test as a curing times function.

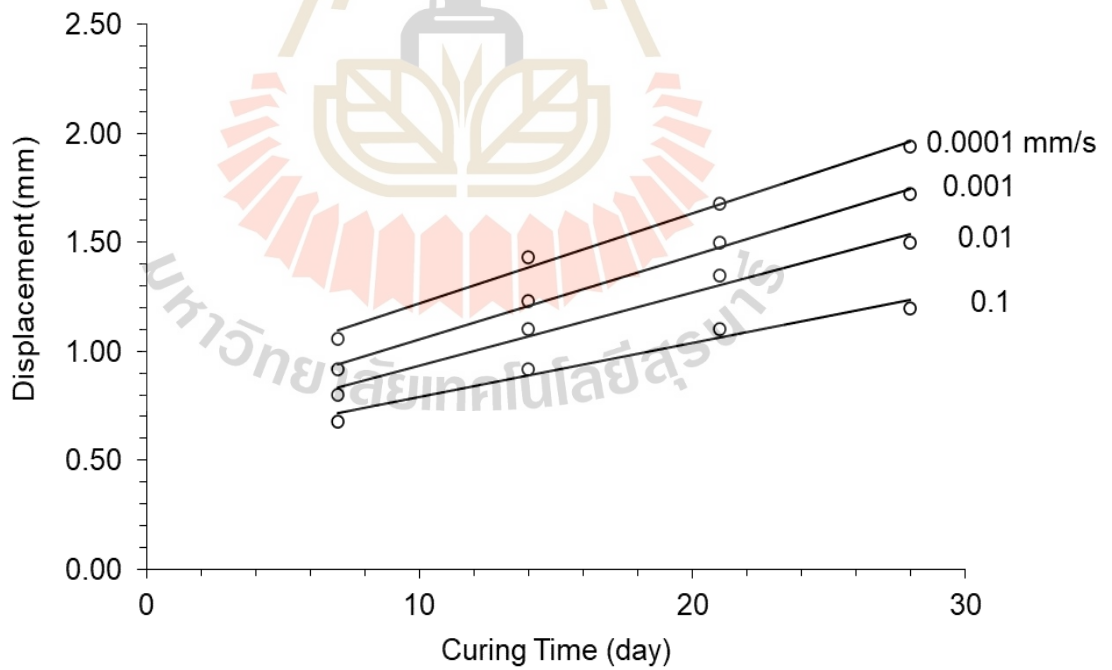


Figure 4.11 Displacement of pull-out test as a curing times function.

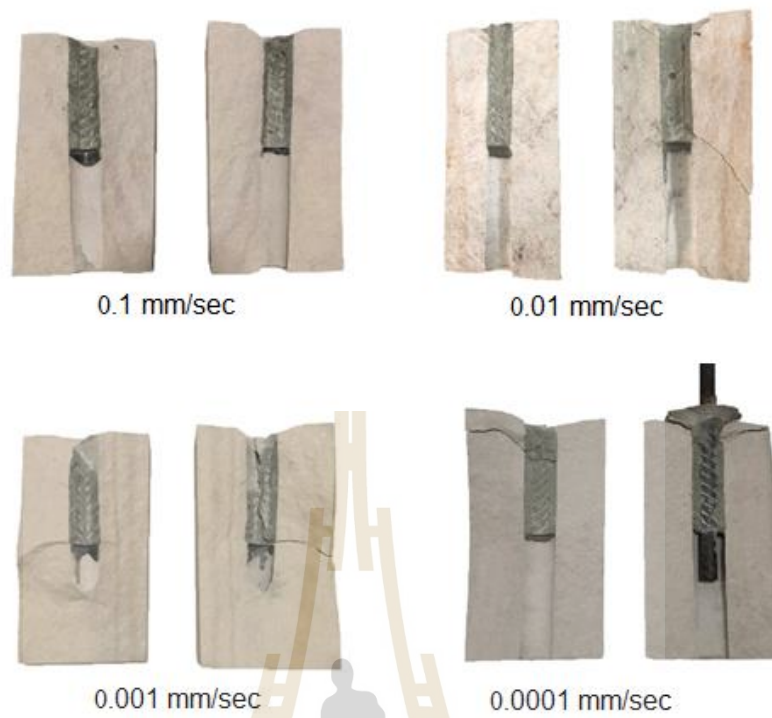


Figure 4.12 Post-test specimens obtained for the 7 days of curing samples under various loading rates.

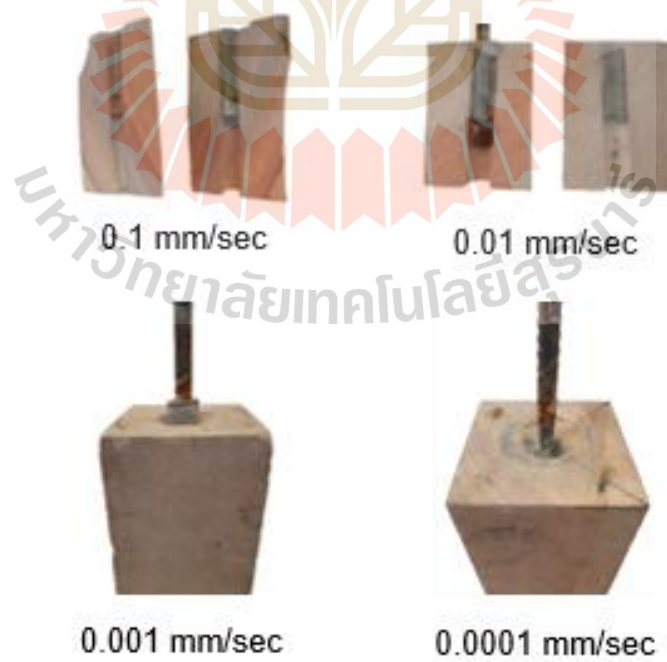


Figure 4.13 Post-test specimens obtained for the 14 days of curing samples under various loading rates.

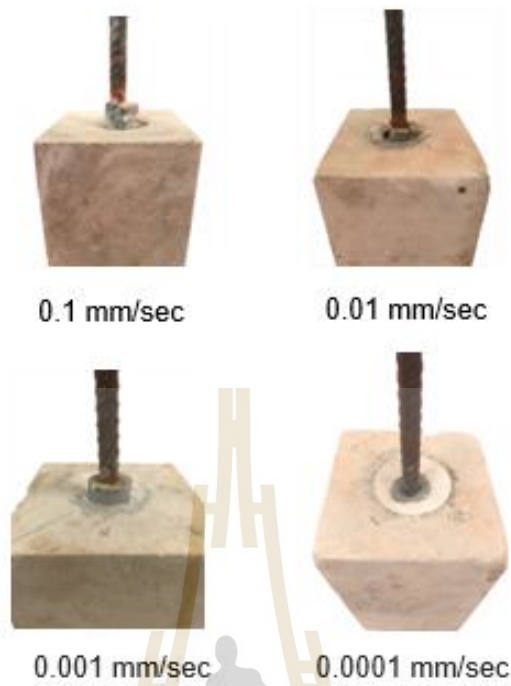


Figure 4.14 Post-test specimens obtained for the 21 days of curing samples under various loading rates.



Figure 4.15 Post-test specimens obtained for the 28 days of curing samples under various loading rates.

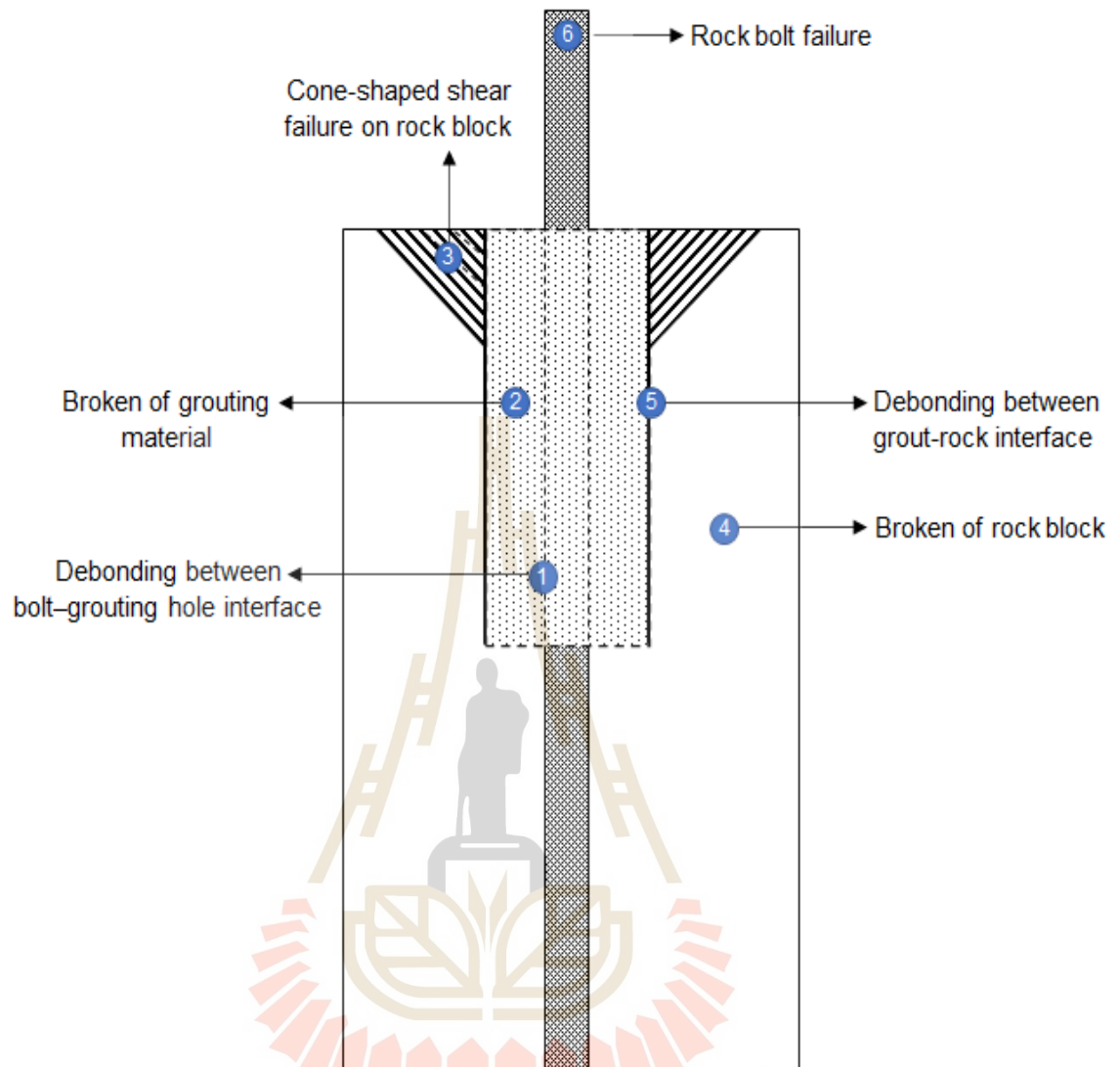


Figure 4.16 Classification of failure modes that can occur during the pull-out test.

Table 4.3 Failure modes observed for the post-test specimens.

Curing time (days)	Loading rate (mm/s)	Mode of failure
7	0.1	1) cone shape shear failure on rock block, 2) broken of grouting material, 3) debonding between bolt-grout interface, and 4) broken of rock block
	0.01	1) cone shape shear failure on rock block, 2) broken of grouting material, 3) debonding between bolt-grout interface, and 4) broken of rock block
	0.001	1) cone shape shear failure on rock block, 2) broken of grouting material, 3) debonding between bolt-grout interface, and 4) broken of rock block
	0.0001	1) cone shape shear failure on rock block, 2) broken of grouting material, 3) debonding between bolt-grout interface, and 4) broken of rock block
14	0.1	1) cone shape shear failure on rock block, 2) broken of grouting material, 3) debonding between bolt-grout interface, and 4) broken of rock block
	0.01	1) cone shape shear failure on rock block, 2) broken of grouting material, 3) debonding between bolt-grout interface, and 4) broken of rock block
	0.001	1) cone shape shear failure on rock block and 2) debonding between grout-rock interface
	0.0001	1) cone shape shear failure on rock block and 2) debonding between grout-rock interface
21	0.1	1) cone shape shear failure on rock block and 2) debonding between grout-rock interface
	0.01	1) cone shape shear failure on rock block and 2) debonding between grout-rock interface
	0.001	1) cone shape shear failure on rock block and 2) debonding between grout-rock interface
	0.0001	1) cone shape shear failure on rock block and 2) debonding between grout-rock interface
28	0.1	1) cone shape shear failure on rock block and 2) debonding between grout-rock interface
	0.01	1) cone shape shear failure on rock block and 2) debonding between grout-rock interface
	0.001	1) cone shape shear failure on rock block and 2) debonding between grout-rock interface
	0.0001	1) cone shape shear failure on rock block and 2) debonding between grout-rock interface

CHAPTER 5

DERIVATION OF EMPIRICAL EQUATIONS

5.1 Introduction

This chapter explains derivation of empirical equations for understanding of pull-out strength and displacement as a function of curing time.

5.2 Pull-out load as a function of curing time

An attempt is made to correlate the pull-out strength with curing time and loading rate. Via regression analysis, their relationship can be expressed in the form of power equation, as follow;

$$P = at^b \quad (5.1)$$

Where P is pull-out load at maximum load. a and b are the empirical parameters. t is curing time. A good correlation is obtained ($R^2 > 0.9$). It should be noted that the pull-out strength depends on the loading rate because the highest loading rate distributes force in the material less than the lowest loading rate leading to receivables' high strength at the highest loading rate before material occurs the failure and deformation (Abdullah, 2021; Fu, et al., 1991; Sriapai, et al., 2011). Pull-out strengths start to rise approximately linearly with curing time. This may be due to the hydration reaction obtained from Elkhadiri et al. (2009) and Rübner et al. (2010) that cement grout in the first 7 days has been compressive strength of approximately 80% of cured 28 days, and slightly increases until complete 28 days. The bonding force between rock bolt-grout material and grout material-grouting hole surface increases pull-out strength with steadily increased value from 7 to 28 days. The parameters a and b are the direct variations relating to the loading rate (\dot{d}_s) follows the below equation:

$$a = \alpha \ln (\dot{d}_s) + \gamma \quad (5.2)$$

$$b = \delta \dot{d}_s^\varepsilon \quad (5.3)$$

where α , γ , δ , and ε are the empirical constants. Substituting Eq. (5.2) and (5.3) into (5.1), the peak load as a function of curing time under various loading rates can be obtained:

$$P = [\alpha \ln (\dot{d}_s) + \gamma] t^{\delta \dot{d}_s^\varepsilon} \quad (5.4)$$

The empirical constants consist of $\alpha = 2.086$, $\gamma = 26.559$, $\delta = 0.333$, and $\epsilon = -0.065$. Figure 5.1 compares the curves of equation (5.4) that fit with the test results. The equation gives the increase of peak load with increasing curing time and loading rate. The peak load has been the value of 0 kN when the curing time is zero-day or before cement setup (cement paste) relates with the good correlation = 0.993.

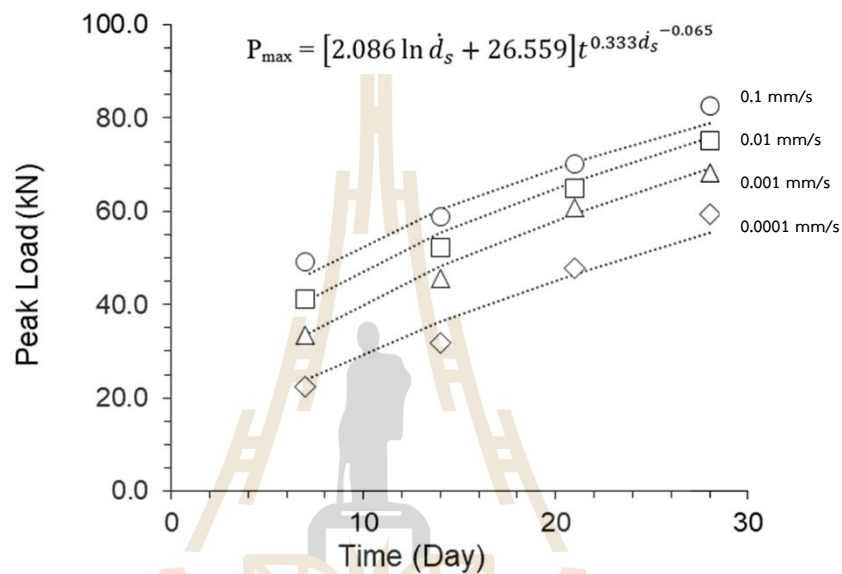


Figure 5.1 Comparison peak load between pull-out test and empirical equation as a curing time function.

5.3 Displacement as a function of curing time

The empirical equation presents the results in form of regression analysis. The displacement of the pull-out test is subjected to the function of curing time and loading rate that is indicated by this relationship of power equation with the correlation coefficients of greater than 0.9.

$$D = ct^e \quad (5.5)$$

Where D is the pull-out displacement at the failure point. c and e are the empirical parameters, and t is curing time. The displacement decreases with increasing of loading rate, this is probably due to the material cannot deform on time. Although, increasing of curing time increased the hydration reaction and lead to more deformation. The parameter c and e relate the direct variation to the loading rate (\dot{d}_s) follows the below equation:

$$c = \zeta \ln(\dot{d}_s) + \kappa \quad (5.6)$$

$$e = \lambda \dot{d}_s^\theta \quad (5.7)$$

where ζ , κ , λ , and θ are empirical constants. Substituting Eq. (5.6) and (5.7) into (5.5) the displacement as a function of curing time and loading rates can be obtained:

$$D = [\zeta \ln(\dot{d}_s) + \kappa] t^{\lambda \dot{d}_s^\theta} \quad (5.8)$$

Empirical constants are $\zeta = -0.026$, $\kappa = 0.213$, $\lambda = 0.463$ and $\theta = 0.008$. The displacement in Equation (5.8) is showed in form logarithm and power equation that compared curve of test result in Figure 5.2. The result of empirical equation of increasing displacement when loading rate decreases and curing time increases value. The equation gives the relation as function curing time and loading rate with the very good correlation = 0.998.

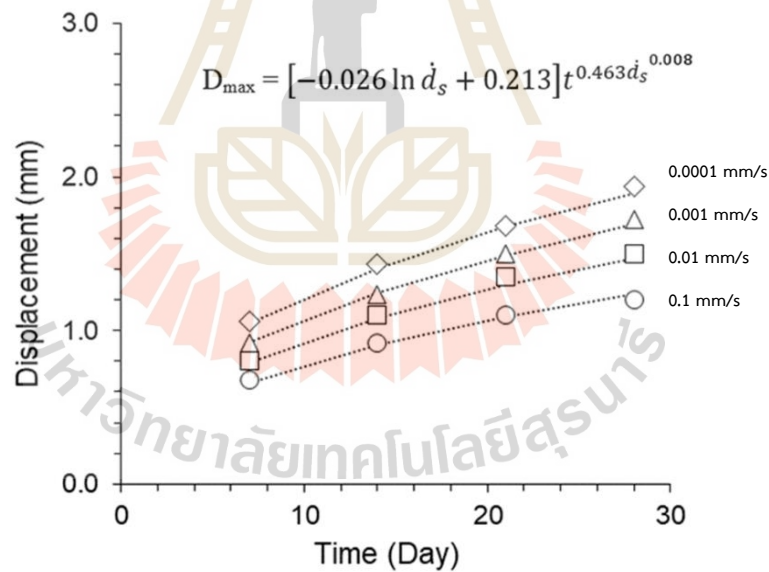


Figure 5.2 Comparison displacement between pull-out test and empirical equation as a curing time function.

CHAPTER 6

DISCUSSIONS, CONCLUSIONS, AND RECOMMENDATIONS FOR FUTURE STUDIES

6.1 Discussions

This section discusses the issues relevant to the reliability of the test schemes and the adequacy of the test results. Comparisons of the results and findings from this study with those obtained elsewhere under similar test conditions have been made. The mechanical properties of the grouting material prepared for the study are examined. The pull-out testing to assess the performance of rock bolts was carried out in the laboratory. The rectangular rock blocks were used to represent the rock mass. The drilling hole in the middle of rock blocks simulated the hole where the rock bolt would be installed. This study focuses on the effect of loading rate on the maximum pull-out load of rock bolt.

The grouting materials are a mixture of Portland cement Type 1 and clean sand. The ratio of the cement and sand (C:S) is constant at 1:1 water-cement (W:C) ratio of 1:0.45 by weight. The grouting material was placed in the 54 mm PVC mold and cured under water at ambient temperature for 3, 7, 14, and 28 days before testing. The results showed that the uniaxial compressive strength of the grout material increased rapidly during the first 7 days (approximately 80% of the samples cured at 28 days) and then tended to increase slightly with time. This is due to the increase of hydration between cement and water as time increases, which agrees well with the test results obtained from Elkhadiri et al. (2009) and Rübner et al. (2010). The modulus of elasticity of the grouting material tended to remain constant at 6.8 GPa, while the Poisson's ratio decreased with increasing curing time. Therefore, the grout material is more resistant to deformation when the compressive strength increases with increasing curing time.

To study the effect of loading rate on the maximum pull-out load of rock bolt, the rectangular rock block with nominal dimension of $110 \times 110 \times 200 \text{ mm}^3$ were prepared from Phra Wihan sandstone to represent the rock mass around the excavation which required to install the rock bolt. These rock specimens have a uniaxial compressive strength of 54 MPa and tensile strength of 6.7 MPa. The elastic and Poisson's ratio are 10.8 GPa and 0.23, respectively. The cohesion and internal friction angle for the Coulomb's strength criterion can be determined as 3.1 MPa and 46 degrees, respectively (Fuenkajorn and Kenkhunthod, 2010; Kapang et al., 2013; Phueakphum et al., 2013). A pre-drilling hole along the center of rock specimens with a diameter of 25 mm was used to install a 12-mm diameter rock bolt (DB12) with grouting material. The

embedment length of rock bolt is approximately 100 mm in the grout material. The ratio of the hole diameter to rock bolt diameter (D_h/D_b) is approximately 2, representing a grout thickness of 6.5 mm. The pull-out tests were conducted on the specimens under four different curing periods (7, 14, 21, and 28 days) and pull-out rates (0.1, 0.01, 0.001, and 0.0001 mm/sec) in accordance with the ASTM Standard practice.

The results show that the ultimate pull-out load increased with increasing curing time and loading rate. This is due to the increase in curing time yielding the grout material to gain its strength as stated above. In addition, the bonding force between the grouting hole surface and grout material and between the grout material and rock bolt gained with time. Of course, the increasing of loading rate will increase the strength of rock and grout material (Abdullah, 2021; Fu, et al., 1991; Sriapai, et al., 2011). It can also be stated that bolt system should not be subjected to stress before 28 days to allow complete hydration reactions. The displacements of the bolt reinforcement system induced by the expansion of the rock bolt during subjected to pull-out load, the deformation of grouting material along the axial load, the slip along the contact surface of rock bolt and grouting material, and between grouting material and grouting hole wall. The results in the study found that the displacement rock bolt reinforcement system increased with curing time and decreased with an increase in loading rate. The highest displacement value can be obtained for the sample with long-term curing sample (28 days) and lowest loading rate (0.0001 mm/sec).

Based on the laboratory experiment, the ultimate failure of the bolts reinforcement system may occur: (a) in the rock bolt, (b) in the grouting material, (c) in the rock block (representing the rock mass), (d) at the bolt-grout interface, (e) at the grout-rock interface, and (f) a combination of these failure modes (Ren, et al. 2010). In this study, the failures of the bolts reinforcement system are a combination. The cone-shaped shear zone develops near the outer boundary of rock block can be obtained for all test conditions. The higher compressive stresses and deeper distribution in the compression zone at the outer surface of the rock block can be obtained for sample when it was tested under a low pull-out rate on longer curing time. As a result, the pull-out test under low pull-out rate (0.0001 mm/s) for high strength of grout material (curing 28 days) yield wider and deeper conical shear zone than those obtained under a high pull-out rate (0.1 mm/s) on low strength of grout material (curing 7 days).

The pull-out test on short curing time sample (at 7 days) for all loading yields the failure in form of the slip between bolt-grout interface, the broken splitting into two pieces and the narrow cone-shaped shear zone develops near the outer boundary of rock block. This is due to this test condition, grout material has a low compressive strength and the adhesive force between bolt and grout material is still low, resulting

in the slip between bolt–grout interface. In addition, while the elastic modulus of the grout material was constant, the Poisson's ratio in this condition (curing at 7 days) was high, which caused a high lateral expansion due to the axial load. The expansion of the grout material results in tangential stress exceeding the rock's tensile strength and eventually breaking the rock sample. Moreover, increasing strength of grouting material increases shear strength obtained from Al-Quraishy (2018) and Wang et al. (2020). If the compressive strength of grouting material is more than the rock sample, that shear strength of grouting material will be increasing more than the rock sample. The opportunity of failure mode with debonding of grout-rock interface will have a very high chance when shear strength of rock sample and grout-rock have been greater difference and slightly less when it's little difference which leads to broken of rock block failure combined with cone shape shear zone which has effect as function of curing time and loading rate following above reason where shear strength of grout-rock interface more than or equal of rock sample and less than grouting material.

6.2 Conclusions

The effect of the pull-out rate and curing time of grouting material (mortar) on the pull-out capacity of fully grouted rock bolts have been experimentally investigated. The effort involves the laboratory test on the compressive strength of cylindrical grouted specimens under various curing periods, a pull-out test on the specimens under different pull-out rates and curing times, and the development of the mathematical relation of pull-out strength that can incorporate the curing time and pull-out rate. The following conclusions are as follows.

1. Uniaxial compressive strength of the grout material increases rapidly during the first 7 days and tends to increase slightly with time. The elastic modulus tends to remain constant as 6.8 GPa, while the Poisson's ratio decreased with increasing curing time.
2. Ultimate pull-out load increases with increasing curing time and loading rate. It can also be stated that rock bolt systems should not be subjected to stress before 28 days.
3. Mathematical relationship proposed here can be used to determine the ultimate pull-out load for such loading rate and curing time.
4. Displacements of the rock bolt reinforcement systems increase with curing time and decrease with an increase of loading rate. The highest displacement value can be obtained for the sample with long-term curing sample (28 days) and lowest loading rate (0.0001 mm/s).

5. Failure mode of the pull-out test includes in two types: cement-bolt zone and cement-rock zone which the most failure starts to occur at least 14 days of curing times with a loading rate equal to or more than 0.01 mm/s.
6. Cone-shaped shear zone develops near the outer boundary of rock block can be obtained for all test conditions. Under low pull-out rate on high strength of grout material give a wider conical shear zone than those obtained under a low pull-out rate and low strength of grout material.

6.3 Recommendations for the future studies

The uncertainties and adequacies of the research investigation and results discussed above lead to recommendations for future studies, as follows.

1. Pull-out tests obtained here that conducted on the specimen without confining pressure, which can make a rock block break out while applying the pull-out load and may result in lower ultimate pull-out loads than those obtained under confining pressure condition. The test should be performed under confining pressure to represent the real in-situ stress condition around the drilling hole.
2. Uniaxial compression test on the cement grout is performed under loading rate conditions (10 N/sec) while the pull-out test of the bolts reinforcement system is conducted under strain rate conditions. The mechanical properties obtained from the uniaxial compression tests in this research may not reflect the actual mechanical properties of cement grout, which are subjected to various loading rates. Therefore, the uniaxial compressive strength test on the cement grout should be performed under various strain rates of 0.0001, 0.001, 0.01, 0.1 mm/sec, respectively.
3. Due to many limitations, only one sample was tested in this study for each test condition (each loading rate for such curing time). Therefore, at least three samples should be tested for each test condition to verify the validity of the test results.
4. Experiment study should be performed to assess the shear strength between rock - cement grout and cement grout - bolt interfaces for such loading rate and curing time. In addition, more displacement points should be measured, such as, at rock bolt, both sides of grout material, elongation of rock bolt, etc. The results can be used to analyze the behavior of the bolts reinforcement system.

REFERENCES

- Abdullah, A. I. (2021, May). Effects of loading rates on concrete compressive strength. In *IOP Conference Series: Materials Science and Engineering* (Vol. 1144, No. 1, p. 012033). IOP Publishing.
- Alaoud, L., Al-Salloum, Y., and Abbas, H. (2021). Experimental investigation for GFRP rebar couplers for reinforced concrete. *Journal of King Saud University-Engineering Sciences*. 33(2): 104-110.
- Al-Quraishy, Q. A. (2018). Behavior of Normal, High and Ultrahigh Strength Concrete in Direct shear. *International Journal of Civil Engineering and Technology (IJCIET)*. 99(2): 349-359.
- Ansell Anders. (2006). Dynamic testing of steel for a new type of energy absorbing rock bolt. *Journal of Constructional Steel Research*. 62(5): 501-512.
- ASTM C150-07. (2009). Standard Specification for Portland Cement. *Annual Book of ASTM Standards* (Vol. 04.01). ASTM International.
- ASTM D4435-13e1. (2014). Standard test methods for rock bolt anchor pull test. *Annual Book of ASTM Standards* (Vol. 04.08). Pennsylvania: American Society for Testing and Materials.
- ASTM International. (2014). D 7012-14 standard test methods for compressive strength and elastic moduli of intact rock core specimens under varying states of stress and temperatures.
- Bazant, Z. P., and Sener, S. (1988). Size effect in pullout tests. *ACI Materials Journal*. 85(5): 347-351.
- Benmokrane, B., Chennouf, A., and Mitri, H. S. (1995). Laboratory evaluation of cement-based grouts and grouted rock anchors. *International Journal of Rock Mechanics and Mining Sciences and Geomechanics Abstracts*. 32(7): 633-642. Pergamon.
- Boshoff, W. P., and Van Zijl, G. P. (2007). Time-dependent response of ECC: Characterisation of creep and rate dependence. *Cement and Concrete Research*. 37(5): 725-734.
- Boshoff, W. P., Mechtcherine, V., and van Zijl, G. P. (2009). Characterising the time-dependant behavior on the single fibre level of SHCC: Part 2: The rate effects on fibre pull-out tests. *Cement and Concrete Research*. 39(9): 787-797.

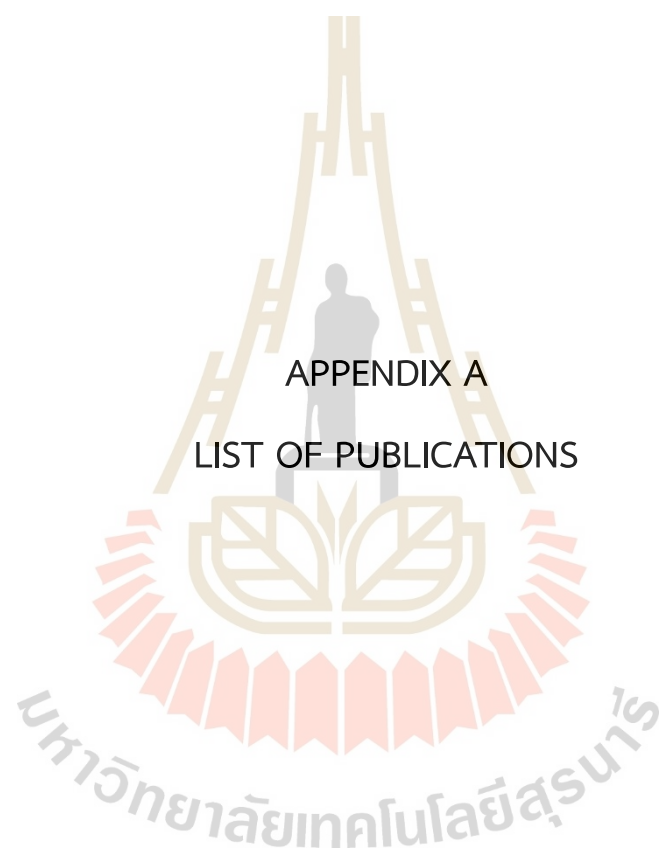
- Che, N., Wang, H., and Jiang, M. (2020). DEM investigation of rock/bolt mechanical behaviour in pull-out tests. *Particuology*. 52: 10-27.
- Chen, Y. (2014). Experimental study and stress analysis of rock bolt anchorage performance. *Journal of Rock Mechanics and Geotechnical Engineering*. 6(5): 428-437.
- Chen, Y., and Li, C. C. (2015). Performance of fully encapsulated rebar bolts and D-Bolts under combined pull-and-shear loading. *Tunnelling and Underground Space Technology*. 45: 99-106.
- Cunha, V. M., Barros, J. A., and Sena-Cruz, J. M. (2010). Pullout behavior of steel fibers in self-compacting concrete. *Journal of Materials in Civil Engineering*. 22(1): 1-9.
- Dai, L., Pan, Y., and Wang, A. (2018). Study of the energy absorption performance of an axial splitting component for anchor bolts under static loading. *Tunnelling and Underground Space Technology*. 81: 176-186.
- Douglas, K. S., and Billington, S. L. (2005). Rate dependence in high-performance fiber reinforced cementbased composites for seismic applications. In *Proceedings, HPRCC-2005 International Workshop*. Honolulu, Hawaii, America.
- Eligehausen, R., Popov, E. P., and Bertero, V. V. (1982). Local bond stress-slip relationships of deformed bars under generalized excitations.
- Elkhadiri, I., Palacios, M., and Puertas, F. (2009). Effect of curing temperature on hydration process of different cement. 53(2): 65-75.
- Federal Energy Regulatory Commission. (2002). Engineering guidelines for the evaluation of hydropower projects, chapter III: gravity dams. *Federal Energy Regulatory Commission*. Washington.
- Feng, X., Zhang, N., Li, G., and Guo, G. (2017). Pullout test on fully grouted bolt sheathed by different length of segmented steel tubes. *Shock and Vibration*. China.
- Franklin, J.A. et al. (1974). ISRM Suggested Methods for Rockbolt Testing. Document No.2 of the committee on field tests (Final draft). *Rock Characterization, Testing and Monitoring* (pp. 163-166). Pergamon Press, Oxford.
- Frenelus, W., Peng, H., and Zhang, J. (2022). An insight from rock bolts and potential factors influencing their durability and the long-term stability of deep rock tunnels. *Sustainability*. 14(17): 10943.
- Fu, H. C., Erki, M. A., and Seckin, M. (1991). Review of effects of loading rate on concrete in compression. *Journal of Structural Engineering*. 117(12): 3645-3659.

- Fuenkajorn, K., and Kenkhunthod, N. (2010). Influence of loading rate on deformability and compressive strength of three Thai sandstones. *Geotechnical and Geological Engineering*. 28: 707-715.
- Ghazvinian, A. H., and Rashidi, M. (2010). Study of the Effect of Ratio of Hole Diameter to Rock Bolt Diameter on Pullout Capacity of Fully Grouted Rock Bolts. *Journal of Rock Mechanics and Tunnelling Tech*. 16(1): 11-18.
- Hao, Y., Wu, Y., Ranjith, P. G., Zhang, K., Hao, G., and Teng, Y. (2020). A novel energy-absorbing rock bolt with high constant working resistance and long elongation: Principle and static pull-out test. *Construction and Building Materials*. 243: 118231.
- Hoek, E., and Wood, D. F. (1988). Rock support. *Mining Magazine*. 159(4): 282-287.
- Høien, A. H., Li, C. C., and Zhang, N. (2021). Pull-out and critical embedment length of grouted rebar rock bolts-mechanisms when approaching and reaching the ultimate load. *Rock Mechanics and Rock Engineering*. 54: 1431-1447.
- Hyett, A. J., Bawden, W. F., and Reichert, R. D. (1992, September). The effect of rock mass confinement on the bond strength of fully grouted cable bolts. In *International Journal of Rock Mechanics and Mining Sciences & Geomechanics abstracts* (Vol. 29, No. 5, pp. 503-524).
- Jayasree, C., and Gettu, R. (2008). Experimental study of the flow behaviour of superplasticized cement paste. *Materials and Structures*. 41(9): 1581-1593.
- Ji, T., Chen, B. C., Zhuang, Y. Z., Li, F., Huang, Z. B., and Liang, Y. N. (2011). Effects of sand particle size and gradation on strength of reactive powder concrete. In *Advanced Materials Research*. 261: 208-211. Trans Tech Publications Ltd.
- joo Kim, D. (2009). Strain rate effect on high performance fiber reinforced cementitious composites using slip hardening high strength deformed steel fibers. University of Michigan.
- Kang, S. H., Kim, J. J., Kim, D. J., and Chung, Y. S. (2013). Effect of sand grain size and sand-to-cement ratio on the interfacial bond strength of steel fibers embedded in mortars. *Construction and Building materials*. 47: 1421-1430.
- Kapang, P., Walsri, C., Sriapai, T., and Fuenkajorn, K. (2013). Shear strengths of sandstone fractures under true triaxial stresses. *Journal of Structural Geology*. 48: 57-71.
- Kilic, A., Yasar, E., and Celik, A. G. (2002). Effect of grout properties on the pull-out load capacity of fully grouted rock bolt. *Tunnelling and Underground Space Technology*. 17(4): 355-362.

- Kim, H., Rehman, H., Ali, W., Najji, A. M., Kim, J. J., Kim, J., and Yoo, H. (2019). Classification of factors affecting the performance of fully grouted rock bolts with empirical classification systems. *Applied Sciences*. 9(22): 4781.
- Komurlu, E., and Demir, S. (2019). Length Effect on Load Bearing Capacities of Friction Rock Bolts. *Periodica Polytechnica Civil Engineering*. 63(3): 718-725.
- Laldji, S., and Young, A. G. (1988). Bond between steel strand and cement grout in ground anchorages. *Magazine of Concrete Research*. 40(143): 90-98.
- Li, C. C. (2010). A new energy-absorbing bolt for rock support in high stress rock masses. *International Journal of Rock Mechanics and Mining Sciences*. 47(3): 396-404.
- Li, C. C. (2011, October). Dynamic test of a high energy-absorbing rock bolt. In *12th ISRM Congress*. OnePetro.
- Li, C. C., Kristjansson, G., and Høien, A. H. (2016). Critical embedment length and bond strength of fully encapsulated rebar rockbolts. *Tunnelling and Underground Space Technology*. 59: 16-23.
- Li, F., Quan, X., Jia, Y., Wang, B., Zhang, G., and Chen, S. (2017). The experimental study of the temperature effect on the interfacial properties of fully grouted rock bolt. *Applied Sciences*. 7(4): 327.
- Littlejohn, G. S., and Bruce, D. A. (1975). Rock anchors-state of the art. Part 1: design. *Ground Engineering*. 8(3).
- Long, X., Wang, C. Y., Zhao, P. Z., and Kang, S. B. (2020). Bond strength of steel reinforcement under different loading rates. *Construction and Building Materials*. 238: 117749.
- Lutz, L. A. (1970, October). Analysis of stresses in concrete near a reinforcing bar due to bond and transverse cracking. In *Journal Proceedings* (Vol. 67, No. 10, pp. 778-787).
- Maalej, M., Quek, S. T., and Zhang, J. (2005). Behavior of hybrid-fiber engineered cementitious composites subjected to dynamic tensile loading and projectile impact. *Journal of Materials in Civil Engineering*. 17(2): 143-152.
- MacSporran, G. R. (1994). An empirical investigation into the effects of mine induced stress change on standard cable bolt capacity.
- Minova (2006). The MINOVA Guide to Resin-Grouted Rockbolts. Minova International Limited.
- Moosavi, M., and Bawden, W. F. (2003). Shear strength of Portland cement grout. *Cement and Concrete Composites*. 25(7): 729-735.
- Mousavi, T., and Shafei, E. (2019). Impact response of hybrid FRP-steel reinforced concrete slabs. *In Structures*. 19: 436-448.

- Nieuwoudt, P. D., and Boshoff, W. P. (2017). Time-dependent pull-out behaviour of hooked-end steel fibres in concrete. *Cement and Concrete Composites*. 79: 133-147.
- Phueakphum, D., Fuenkajorn, K., and Walsri, C. (2013). Effects of intermediate principal stress on tensile strength of rocks. *International Journal of Fracture*. 181(2): 163-175.
- Prokeš, J., Girgle, F., Zlámal, M., Čairovič, Đ., Štěpánek, P., and Čechmánek, R. (2020). Application of the FRP rebar in constructions for reduction of thermal bridges– Behavior of compressed elements at room and elevated temperatures. In *AIP Conference Proceedings* (Vol. 2210, No. 1). Brno, Czech.
- Qasem, A., Sallam, Y. S., Eldien, H. H., and Ahangarn, B. H. (2020). Bond-slip behavior between ultra-high-performance concrete and carbon fiber reinforced polymer bars using a pull-out test and numerical modelling. *Construction and Building Materials*. 260: 119857.
- Ren, F. F., Yang, Z. J., Chen, J. F., and Chen, W. W. (2010). An analytical analysis of the full-range behaviour of grouted rockbolts based on a tri-linear bond-slip model. *Construction and Building Materials*. 24(3): 361-370.
- Roussel, N., and Le Roy, R. (2005). The Marsh cone: a test or a rheological apparatus?. *Cement and Concrete Research*. 35(5): 823-830.
- Rübner, K., Meng, B., and Müller, U. (2010). Investigating the original water content of concrete. *Non-destructive evaluation of reinforced concrete structures*. 1: 217-241. Woodhead Publishing.
- Sriapai, T., Samsri, P., and Fuenkajorn, K. (2011). Loading Rate Effects on Compressive Strength of Maha Sarakham Salt. *Engineering Journal of Research and Development*. 22(4): 43-50.
- Stille, H., Holmberg, M., and Nord, G. (1989, January). Support of weak rock with grouted bolts and shotcrete. *International Journal of Rock Mechanics and Mining Sciences and Geomechanics Abstracts*. 26(1): 99-113. Pergamon.
- Stocker, M. F., and Sozen, M. A. (1969). Bond characteristics of prestressing strand, Teil VI von Investigation of prestressed reinforced concrete for Highway bridges. *University of Illinois Structural Research Series*. (344).
- Tahmasebinia, F., Zhang, C., Canbulat, I., Vardar, O., and Saydam, S. (2018). Numerical and analytical simulation of the structural behaviour of fully grouted cable bolts under impulsive loading. *International Journal of Mining Science and Technology*. 28(5): 807-811.

- Takeda, J. I. (1984). Dynamic fracture of concrete structures due to severe earthquakes and some consideration on countermeasures. In *Proceedings of the 8th World Conference on Earthquake Engineering* (pp. 299-306). San Francisco, California, America.
- Thenevin, I., Blanco-Martín, L., Hadj-Hassen, F., Schleifer, J., Lubosik, Z., and Wrana, A. (2017). Laboratory pull-out tests on fully grouted rock bolts and cable bolts: Results and lessons learned. *Journal of Rock Mechanics and Geotechnical Engineering*. 9(5): 843-855.
- Wang, Y., Xiong, Z. Q., Wang, C., Su, C. D., and Li, X. F. (2020). Research on the Reasonable Grouting Strength of Rock-Like Samples in Different Strengths. *Materials*. 13(14): 3161.
- Wang, Z., Zhao, Y., Li, F., and Jiang, J. (2013). Extreme dynamic responses of mw-level wind turbine tower in the strong typhoon considering wind-rain loads. *Mathematical Problems in Engineering*.
- Wu, X., Jiang, Y., Guan, Z., and Wang, G. (2018). Estimating the support effect of energy-absorbing rock bolts based on the mechanical work transfer ability. *International Journal of Rock Mechanics and Mining Sciences*. 103: 168-178.
- Yahia, A. (2011). Shear-thickening behavior of high-performance cement grouts— Influencing mix-design parameters. *Cement and Concrete Research*. 41(3): 230-235.
- Yang, E., and Li, V. C. (2006). Rate dependence in engineered cementitious composites. *International RILEM Workshop on High Performance Fiber Reinforced Cementitious Composites in Structural Applications* (pp. 83-92).
- Yang, H. (2022). Experimental Study on Mechanical Properties of Fully Bonded Bolts with Varied Bond Length. *Geotechnical and Geological Engineering*. 40(8): 4083-4094.
- Yoo, D. Y., and Banthia, N. (2015). Numerical simulation on structural behavior of UHPFRC beams with steel and GFRP bars. *Computers and Concrete*. 16(5): 759-774.
- Zhai, H., Hagan, P., and Li, D. (2016). Sample Size and Sample Strength Effects on Testing the Performance of Cable Bolts. *Proceedings of the 16th Coal Operators' Conference* (pp. 40-52). Mining Engineering, University of Wollongong.
- Zhang, C., Cui, G., Chen, X., Zhou, H., and Deng, L. (2020). Effects of bolt profile and grout mixture on shearing behaviors of bolt-grout interface. *Journal of Rock Mechanics and Geotechnical Engineering*. 12(2): 242-255.
- Zhao, T. B., Guo, W. Y., Yin, Y. C., and Tan, Y. L. (2015). Bolt pull-out tests of anchorage body under different loading rates. *Shock and Vibration*.



APPENDIX A
LIST OF PUBLICATIONS

LIST OF PUBLICATIONS

Apichaibukkhon, P., Phueakphum, D., and Fuenkajorn, K. (2023). Pull-out test of grouted rock bolt as affected by loading rate and curing time. In *Proceedings of Academicsera International Conference*, 27th - 28th May, 2023 (pp.1-7). Ottawa, Canada.



PULL-OUT TEST OF GROUTED ROCK BOLT AS AFFECTED BY LOADING RATE AND CURING TIME

¹PIYAWAT APICHAIBUKKHON, ²DECHO PHUEAKPHUM, ³KITTITTEP FUENKAJORN

^{1,2,3} Geomechanics Research Unit, Institute of Engineering, Suranaree University of Technology, Nakhon Ratchasima, 30000, Thailand
E-mail: ¹M6201067_piya@hotmail.com, ²phueakphum@sut.ac.th, ³fuenkajorn@sut.ac.th

Abstract - This study investigated the effects of pull-out rate and curing time on the ultimate load capacity of grouted rock bolts. The laboratory tests include the uniaxial compression test on grouting material and the pull-out test on rock bolts. The compressive strength of grouted cement for curing periods of 3, 7, 14, 21, and 28 days equals 26, 32, 35, 37, and 41 MPa, respectively. The pull-out tests were conducted on the specimens under four different curing periods (7, 14, 21, and 28 days) and pull-out rates (0.1, 0.01, 0.001, and 0.0001 mm/sec) following the ASTM Standard practice. The results indicate that the increasing curing time leads to an increase in pull-out load and displacement, while the effect of loading rate makes for an increased pull-out load but a decreasing displacement. The mathematical equation for the ultimate pull-out load and displacement is presented as a function of loading rate and curing time with correlation coefficients of 0.993 and 0.998, respectively.

Keywords - Pull-Out Test, Effect of Curingtime, Loading Rate, Rock Bolt

I. INTRODUCTION

Rock support has been used in civil and mining projects involving surface and underground excavations in rock masses such as tunnels, rock slopes, and foundations. They are widely used to improve stability and maintain the load-bearing capacity of rock near the excavation boundaries. There are four main types of rock support systems: rock bolts, shotcrete, steel sets, and concrete lining. There are many potential factors affecting the durability and the performance of rock bolts, including rock mass characteristic (strength and creep behavior of rock), bolt parameters (bolt type, tensile strength, elongation, corrosion, bolt length and diameter), grout material (grout types, mixture and water-to-cement ratio), and anchorage system (embedment length, hole diameter to bolt diameter ratio, number of bolts, bolt spacing and orientation of rock bolt) [1]. Many researchers have carried out laboratory tests, field tests, analytical methods, and numerical analysis for a better understanding of rock bolt performance [2-10]. Ghazvinian and Rashidi [2] studied the effect of the hole diameter to rock bolt diameter ratio (D_h/D_b) on the pull-out capacity of fully grouted rock bolts. The results indicate that the increase in the diameter of the hole beyond an optimal limit led to a decrease in the load-bearing capacity. They recommended that the optimum hole diameter should be 1.7 to 1.9 times the rock bolt diameter. If the diameter of the hole is more than the optimum range, considerable reduction (5% to 15%) takes place in the maximum pull-out load.

Li et al. [3] studied the effect of embedment length on the bond strength of fully encapsulated rebar rock bolts under three different water-cement (w/c) ratios. The results indicate that the rock bolts' critical embedment lengths depend on the water-cement

ratio, which corresponds with the cement grout's uniaxial compressive strength (UCS) of cement grout. The critical embedment length is approximately 25, 32, and 36 cm for the cement grout with UCS of 37 MPa (w/c ratio = 0.40), 32 MPa (w/c ratio= 0.46), 28 MPa (w/c ratio = 0.50), respectively. Kilic et al. [11] studied the influence of the diameter and length of rock bolts, grout properties (w/c ratio), and curing time on the pull-out load capacity of fully grouted rock bolts. The results showed that the bolt bearing capacity increased with increasing bolt length and diameter. Increasing the curing time increases the bolt bond strength. The bond strength of grouted bolts decreases with increasing the water-cement ratio. They recommended that the optimum water-to-cement ratio must be 0.34-0.40.

Zhao et al. [12] conducted the numerical simulation using particle flow code software (PFC2D) to study the loading rate's effect on grouted rock bolts' performance. The differential loading rates ranging from 0.5 mm/s to 1000 mm/s are applied to the rock bolt. The results found that high loading rates provide a higher maximum pull-out load. Long et al. [13] investigated the bond strength of steel reinforcement under different loading rates. The results found that the pull-out resistance of steel reinforcement with various embedment lengths was increased by a high loading rate.

Even though several factors have been tested, the performance of cement plugs in rocks as affected by the pull-out rate has been rare and used to prevent hazardous conditions such as the collapse of buildings, tower overturning, or high structures related to tension foundations. This study aims to determine the capacity of grouted rock bolts as affected by the curing time of cement grout and the loading rate applied to the rock bolts. Sixteen conditions were tested with varying

loading rates ranging from 0.1 to 0.0001 MPa/s and curing times ranging from 7 to 28 days. The empirical equations are formulated to present the maximum pull-out load and bolt displacement as a function of curing time and loading rate. These equations have the advantage, which can be used to predict the capacity of grouted rock bolts that are installed to support the engineering structure.

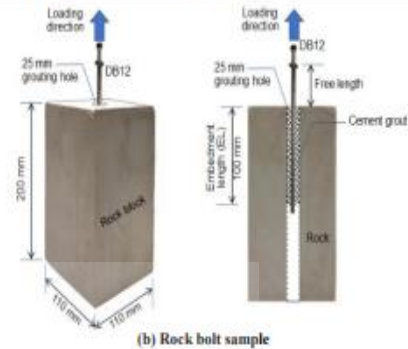
II. SAMPLE PREPARATION

Sandstone specimens with nominal dimensions of $110 \times 110 \times 130 \text{ mm}^3$ were prepared from Phra Wihan sandstone. These rock blocks represent the rock mass around the excavations required to install the rock bolt. The uniaxial compressive strength and tensile strength equals 54 MPa and 6.7 MPa, respectively. The elastic and Poisson's ratio equal 10.8 GPa and 0.23, respectively. The cohesion and internal friction angle for the Coulomb's strength criterion can be determined as 3.1 MPa and 46 degrees, respectively (Fuenkajorn and Kenkhunthod [14], Kapang et al. [15], Phueakphum et al. [16]). A pre-drilling hole along the center of rock specimens with a diameter of 25 mm was used to install a 12-mm diameter rebar bolt (DB12) with cement grouting. The bolt diameter (D_b) to hole diameter (D_h) is approximately 2. This ratio is within the optimum range recommended by Ghazvinian and Rashidi [2].

The cement grout mixture consists of Portland cement Type I, clean sand, and fresh water. They are mixed with a blender machine [17], followed by ASTM C109 [18]. The ratio of cement and sand (C:S) is constant at 1:1 water-cement (W:C) ratio of 0.45:1 by weight. The natural clean sand passed No. 20 and retained the No. 40 sieves with a particle size ranging between 0.425 - 0.850 mm. The cement grout was placed in the 54 mm PVC mold and cured in fresh water at ambient temperature for 3, 7, 14, and 28 days. Then they were tested to determine the uniaxial compressive strength, elastic modulus, and Poisson's ratio. The pull-out test specimens are prepared by pouring the cement grout into the pre-drilling hole where the DB12 is installed with a 100 mm embedment length. They were also cured in fresh water at ambient temperature for 7, 14, 21, and 28 days before the pull-out test. Fig. 1 shows some of the specimens prepared for laboratory tests.



(a) Grouting cement samples



(b) Rock bolt sample

Fig. 1 Some grouting cement samples and rock bolt prepared for laboratory test.

III. LABORATORY TEST

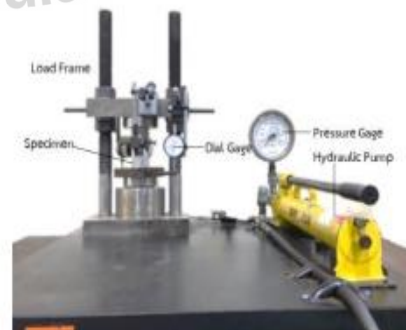
The uniaxial compression test on grouting material and pull-out test on grouted rock bolts are conducted following the ASTM 7012-14 standard practice [19], ASTM D4435 standard practice [20], and ISRM suggested method for rock bolt testing [21], respectively.

A. Uniaxial Compression test

The cylindrical-shaped specimens of the grouting material cured for 3, 7, 14, 21, and 28 days are set up in a load frame and equipped with a hydraulic pump for applying the compression load with a constant stress rate at 1 MPa/s. The axial and radial displacements are measured using four dial gauges (2 gauges for each axial and radial movement) until failure occurs (Fig. 2a).

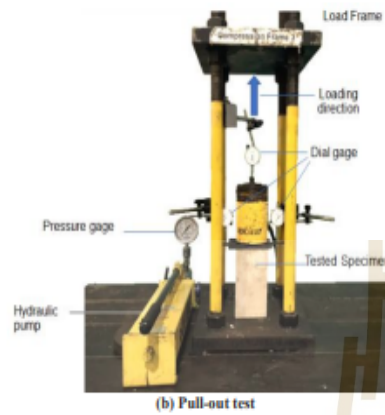
B. Pull-out Test

The pull-out test specimens are equipped with the load cell to generate the pull-out load that induces on the rock bolt. The dial gauges are installed to monitor the displacement of rock bolts (Fig. 2b). The constant pull-out rates vary from 0.1, 0.01, 0.001, and 0.0001 mm/s.



(a) Uniaxial compression test

Pull-Out Test of Grouted Rock Bolt as Affected by Loading Rate and Curing Time



(b) Pull-out test
 Fig. 2 The test apparatus and test set up for the uniaxial compression pull-out tests.

IV. RESULTS AND DISCUSSIONS

A. Uniaxial Compressive test

The compressive stresses (σ , MPa) are calculated by the axial load (P , kN) divided by the specimen area (A , in cm^2). The elastic modulus and Poisson's ratio are calculated from the stress-strain curves. The uniaxial compressive strengths (σ_c), elastic moduli (E), and Poisson's ratio (ν) are plotted as function curing time (Fig.3). The results showed that the uniaxial compressive strength of the grout material increased rapidly during the first seven days (approximately 80% of the samples cured at 28 days) and then tended to increase slightly with time because of the increased hydration reaction between cement and water as time increases, which agrees well with the test results obtained from Elkhadiri et al. [22] and Rübner et al. [23]. The modulus of elasticity of the grouting material tended to remain constant at 6.8 GPa, while the Poisson's ratio decreased with increasing curing time. Therefore, the deformation of grout material has a small value when the compressive strength increases with curing time.

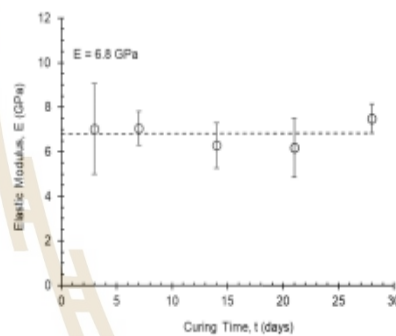
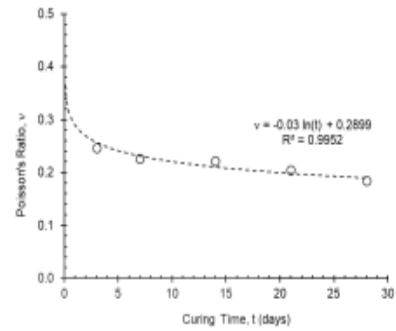
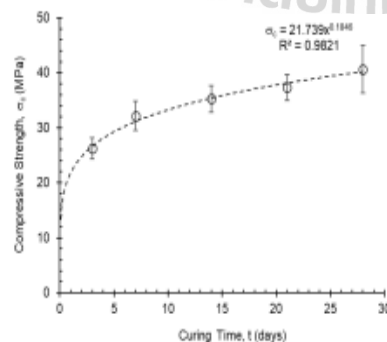


Fig. 3 The compressive strength, Poisson's ratio, and elastic modulus plotted as the function of curing time.

B. Pull-out Test

The pull-out loads are plotted as a function of displacement under different loading rates for such curing time (Fig. 4). The peak load and displacement are plotted in Fig. 5. The results showed that the ultimate pull-out load increased with increasing curing time and loading rate because of increased in curing time yielding the grout material to gain its strength as stated above. In addition, the bonding force between the grouting hole surface and grout material and between the grout material and rock bolt gained with time. Of course, the increasing loading rate will increase the strength of rock and grout material (Abdullah, [24]; Fu, et al., [25]; Sriapai, et al., [26]). It can also be stated that the bolt system should only be subjected to stress after 28 days to allow complete hydration reactions.

The displacements of the rock bolt are the summation of the expansion of the rock bolt during subjected to pull-out load, the deformation of grouting material along the axial load, the slip along the contact surface of the rock bolt and grouting material, and between grouting material and grouting hole wall. The results of the study found that the displacement rock bolt increased with curing time and decreased with an increase in loading rate. The highest displacement

Pull-Out Test of Grouted Rock Bolt as Affected by Loading Rate and Curing Time

value can be obtained for the sample with a long-term curing sample (28 days) and the lowest loading rate (0.0001 mm/sec).

Based on the laboratory experiment, the ultimate failure of the bolts reinforcement system may occur: (a) in the rock bolt, (b) in the grouting material, (c) in the rock block (representing the rock mass), (d) at the bolt-grout interface, (e) at the grout-rock interface, and (f) a combination of these failure modes (Ren, et. al. [27]) as shown in Fig.6. In this study, the failures of the bolts reinforcement system are a combination. Fig. 7 shows the post-test specimens obtained for the 7, 14, 21, and 28 days of curing samples under various loading rates. The cone-shaped shear zone that develops near the outer boundary of the rock block can be obtained for all test conditions. The higher compressive stresses and deeper distribution in the compression zone at the outer surface of the rock block can be obtained for the sample when it was tested under a low pull-out rate on longer curing time. As a result, the pull-out test under a low pull-out rate (0.0001 mm/s) for high strength of grout material (curing 28 days) yields broader and deeper conical shear zone than those obtained under a high pull-out rate (0.1 mm/s) on low strength of grout material (curing seven days).

The pull-out test on a short curing time sample (at seven days) for all loading rates yields the failure in the form of the slip between the bolt-grout interface, broken splitting into two pieces, and the narrow cone-shaped shear zone develops near the outer boundary of rock block. In this test condition, the grout material yields a lower compressive strength and the adhesive force between the bolt and grout material. It results in the slip between the bolt-grout interface. In addition, while the elastic modulus of the grout material was constant, the Poisson's ratio in this condition (curing at seven days) was high, which caused a high lateral expansion due to the axial load. The grout material's expansion can create tangential stress over the rock's tensile strength, eventually breaking the rock sample.

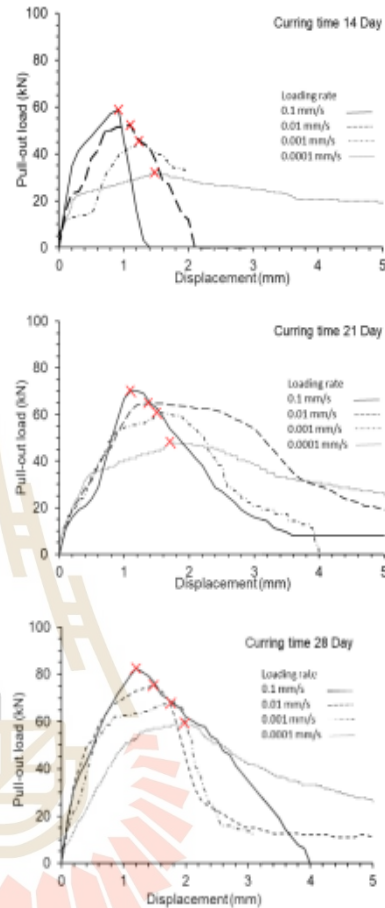
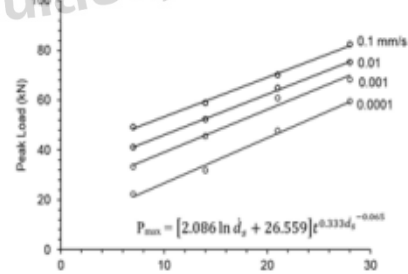
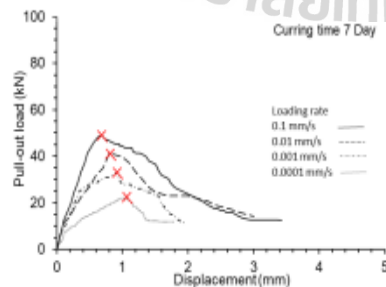
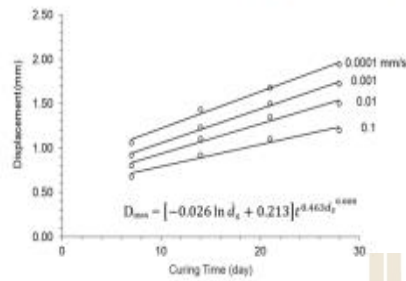


Fig. 4 Load-displacement curve obtained for 7, 14, 21, and 28 days of curing samples under various loading rates. The cross symbols represent the ultimate pull-out load for such loading rate.



Pull-Out Test of Grouted Rock Bolt as Affected by Loading Rate and Curing Time



The empirical equations formulated here can be used to predict the ultimate pull-out load for such loading rate and curing time.

$$P_{max} = [2.086 \ln \dot{d}_s + 26.559] t^{0.333 \dot{d}_s^{-0.065}} \quad (1)$$

$$D_{max} = [-0.026 \ln \dot{d}_s + 0.213] t^{0.463 \dot{d}_s^{0.008}} \quad (2)$$

Where P_{max} is the ultimate pull-out load or maximum peak load (kN), D_{max} is the maximum displacement (mm) at ultimate pull-out load, \dot{d}_s is mean pull-out rate or loading rate (ms^{-1}), and t is curing time (day). The equations (2) and (3) give the correlation coefficients of 0.993 and 0.998, respectively.

Fig.5 The displacement as the curing time function.

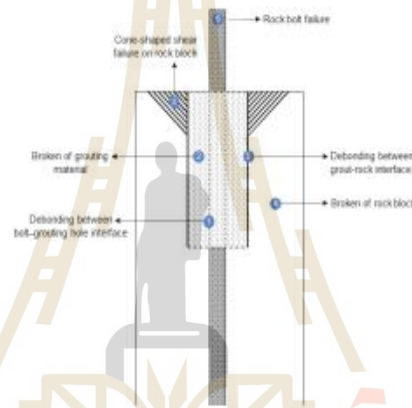


Fig. 6 Classification of failure modes that can occur during the pull-out test.



Fig. 7 Post-test specimens were obtained for the 7, 14, 21, and 28 days of cured samples under various loading rates.

V. CONCLUSION

The effect of the pull-out rate and curing time of grouting material (mortar) on the pull-out capacity of fully grouted rock bolts have been experimentally investigated. The effort involves the laboratory test on the compressive strength of cylindrical grouted specimens under various curing periods, a pull-out test on the specimens under different pull-out rates and curing times, and the development of the mathematical relation of pull-out strength that can incorporate the curing time and pull-out rate. The following conclusions are as follows.

1. The uniaxial compressive strength of the grout material increased rapidly during the first 7 days and then tended to increase slightly with time. The elastic modulus tended to remain constant as 6.8GPa, while the Poisson's ratio decreased with increasing curing time.
2. The ultimate pull-out load increased with increasing curing time and loading rate. It can also be stated that rock bolt systems should not be subjected to stress before 28 days.
3. The mathematical relationship proposed here can be used to determine the ultimate pull-out load for such loading rate and curing time.
4. The displacements of the rock bolt reinforcement systems increased with curing time and decreased with an increase in loading rate. The highest displacement value can be obtained for the sample with long-term curing sample (28 days) and lowest loading rate (0.0001 mm/s).
5. The failure mode of the pull-out test is shown in two types: cement-bolt zone and cement-rock zone which the most failure starts to occur at least 14 days of curing times with a loading rate equal to or more than 0.01 mm/s.
6. The cone-shaped shear zone develops near the outer boundary of rock block can be obtained for all test conditions. Under low pull-out rate on high strength of grout material give a wider conical shear zone than those obtained under a low pull-out rate and low strength of grout material.

ACKNOWLEDGEMENTS

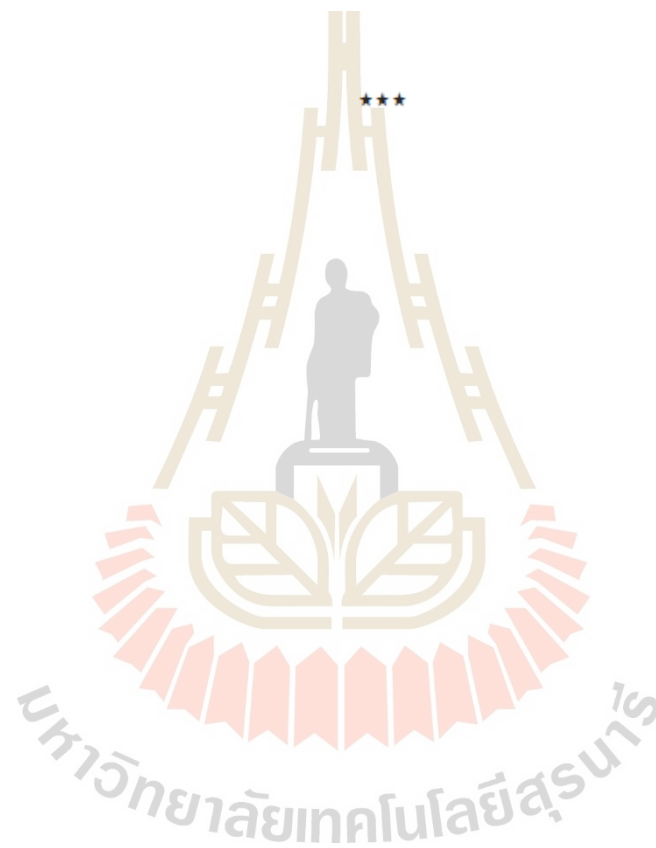
This work was supported by Suranaree University of Technology (SUT) and Thailand Science Research and Innovation (TSRI). Permission to publish this paper is gratefully acknowledged.

REFERENCES

- [1] W. Frenelus, W., Peng, H., and Zhang, J. "An insight from rock bolts and potential factors influencing their durability and the long-term stability of deep rock tunnels." *Sustainability*, 14(17), 10943, 2022.
- [2] A.H. Ghazvinian and M. Rashidi, "Study of the Effect of Ratio of Hole Diameter to Rock Bolt Diameter on Pullout Capacity of Fully Grouted Rock Bolts." *J. Rock Mech. Tun. Tech.*, vol. 16(1), pp. 11-18, 2010.
- [3] C.C. Li, G. Kristjansson, and A.H. Høien, "Critical embedment length and bond strength of fully encapsulated rebar rockbolts." *Tunnelling and Underground Space Technology*, 59, pp. 16-23, 2016.
- [4] Y. Chen, "Experimental study and stress analysis of rock bolt anchorage performance." *Journal of Rock Mechanics and Geotechnical Engineering*, 6(5), pp. 428-437, 2014.
- [5] A.J. Hyett, W.F. Bawden, and R.D. Reichert, "The effect of rock mass confinement on the bond strength of fully grouted cable bolts." In *International journal of rock mechanics and mining sciences & geomechanics abstracts* (Vol. 29, No. 5, pp. 503-524). Pergamon, 1992.
- [6] Y. Chen, and C.C. Li, C., "Performance of fully encapsulated rebar bolts and D-Bolts under combined pull-and-shear loading." *Tunnelling and Underground Space Technology*, 45, pp. 99-106, 2015.
- [7] H. Yang, "Experimental study on mechanical properties of fully bonded bolts with varied bond length." *Geotechnical and Geological Engineering*, 40(8), pp. 4083-4094, 2022.
- [8] C. Zhang, G. Cui, X. Chen, H. Zhou, and L. Deng, "Effects of bolt profile and grout mixture on shearing behaviors of bolt-grout interface." *J. Rock Mech. Geotech. Eng.*, vol. 12(2), pp. 242-255, 2020.
- [9] A.H. Høien, C.C. Li, and N. Zhang, N. "Pull-out and critical embedment length of grouted rebar rock bolts-mechanisms when approaching and reaching the ultimate load." *Rock Mechanics and Rock Engineering*, 54, pp. 1431-1447, 2021.
- [10] F. Li, X. Quan, Y. Jia, B. Wang, G. Zhang, and S. Chen, S. "The experimental study of the temperature effect on the interfacial properties of fully grouted rock bolt." *Applied Sciences*, 7(4), 327, 2017.
- [11] A. Kılıç, E. Yasar, A.G. Celik, "Effect of grout properties on the pull-out load capacity of fully grouted rock bolt." *Tunnelling and Underground Space Technology*, 17(4), pp. 355-362, 2002.
- [12] T.B. Zhao, W.Y. Guo, Y.C. Yin, and Y.L. Tan, "Bolt pull-out tests of anchorage body under different loading rates." *Shock and Vibration*, 2015.
- [13] X. Long, C.Y. Wang, P.Z. Zhao, and S.B. Kang, "Bond strength of steel reinforcement under different loading rates." *Construction and Building Materials*, 238, 117749, 2022.
- [14] K. Fuenkajorn, and N. Kenkhunthod, "Influence of loading rate on deformability and compressive strength of three Thai sandstones." *Geotechnical and Geological Engineering*, vol. 28, pp. 707-715, 2010.
- [15] P. Kapang, C. Walsri, T. Sriapai, and K. Fuenkajorn, "Shear strengths of sandstone fractures under true triaxial stresses." *Journal of Structural Geology*, vol. 48, pp. 57-71, 2013.
- [16] D. Phueakphum, K. Fuenkajorn, and C. Walsri, "Effects of intermediate principal stress on tensile strength of rocks." *International Journal of Fracture*, vol. 181(2), pp. 163-175, 2013.
- [17] ASTM D305-14, Standard Practice for Mechanical Mixing of Hydraulic Cement Pastes and Mortars of Plastic Consistency, West Conshohocken, USA: PA, 2014.
- [18] ASTM C109, Standard Test Method for Compressive Strength of Hydraulic Cement Mortars, West Conshohocken, USA: PA.
- [19] ASTM International. (2014). D 7012-14 standard test methods for compressive strength and elastic moduli of intact rock core specimens under varying states of stress and temperatures.
- [20] ASTM D4435-08, Standard Test Method for Rock Bolt Anchor Pull Test, West Conshohocken, USA: PA, 2008.
- [21] J. A. Franklin, "ISRM suggested methods for rockbolt testing." *Rock Charc. T. Mon.*, 1981.
- [22] I. Elkhadiri, M. Palacios, and F. Puertas, "Effect of curing temperature on hydration process of different cement." vol. 53(2), pp. 65-75, 2009.
- [23] K. Rübner, B. Meng, and U. Müller, "Investigating the original water content of concrete." *Non-destructive evaluation of*

Pull-Out Test of Grouted Rock Bolt as Affected by Loading Rate and Curing Time

- reinforced concrete structures. Woodhead Publishing, pp. 217-241, 2010.
- [24] A. I. Abdullah, "Effects of loading rates on concrete compressive strength," IOP Conference Series: Materials Science and Engineering, vol. 1144, No. 1, p. 012033. IOP Publishing, 2021, May.
- [25] H. C. Fu, M. A. Erki, and M. Seckin, "Review of effects of loading rate on concrete in compression," Journal of structural engineering, vol. 117(12), pp. 3645-3659, 1991.
- [26] T. Sriapai, P. Samsri, and K. Fuenkajom, "Loading Rate Effects on Compressive Strength of Maha Samkham Salt," Engineering Journal of Research and Development, vol. 22(4), pp. 43-50, 2011.
- [27] F. F. Ren, Z. J. Yang, J. F. Chen, and W. W. Chen, "An analytical analysis of the full-range behaviour of grouted rockbolts based on a tri-linear bond-slip model," Construction and Building Materials, vol. 24(3), p.p. 361-370, 2010.



BIOGRAPHY

Mr. Piyawat Apichaibukkhon was born on September 17, 1996 in Muang District, Surin Province, Thailand. He graduated with a bachelor's degree in engineering. (Geological Technology) from the Suranaree University of Technology in 2019. After graduating, he was admitted to a master's degree in Civil, Transportation, and Georesources Engineering Program, the Institute of Engineering, Suranaree University of Technology During graduation in 2022, he was a temporary employee in the Geomechanics Research Unit School of Engineering Suranaree University of Technology

